12. Jacobson S, Shida H, McFarlin DE, Fauci AS, Koenig S (1990) Circulating CD8+ cytotoxic T lymphocytes specific for HTLV-I pX in patients with HTLV-I associated neurological disease. Nature 348: 245–248.
13. Parker CE, Daenke S, Nightingale S, Bangham CR (1992) Activated, HTLV-1-specific cytotoxic T-lymphocytes are found in healthy seropositives as well as in patients with tropical spastic paraparesis. Virology 188: 628–636.
14. Goon PK, Biancardi A, Fast N, Igakura T, Hanon E, et al. (2004) Human T cell lymphotropic virus (HTLV) type-1-specific CD8+ T cells: frequency and immunodominance hierarchy. J Infect Dis 189: 2294–2298.
15. Hanon E, Hall S, Taylor GP, Saito M, Davis R, et al. (2000) Abundant tax protein expression in CD4+ T cells infected with human T-cell lymphotropic virus type I (HTLV-I) is prevented by cytotoxic T lymphocytes. Blood 95: 1386–1392.
16. Satou Y, Yasunaga J, Yoshida M, Matsuoka M (2006) HTLV-I basic leucine zipper factor gene mRNA supports proliferation of adult T cell leukemia cells. Proc Natl Acad Sci U S A 103: 720–725.
17. Macnamara A, Rowan A, Hilburn S, Kadolsky U, Fujiwara H, et al. (2010) HLA class I binding of HBZ determines outcome in HTLV-1 infection. PLoS Pathog 6: e1001117.
18. Hilburn S, Rowan A, Demontis MA, MacNamara A, Asquith B, et al. (2011) In vivo expression of human T-lymphotropic virus type 1 basic leucine-zipper protein generates specific CD8+ and CD4+ T-lymphocyte responses that correlate with clinical outcome. J Infect Dis 203: 529–536.
19. Landry S, Halin M, Vargas A, Lemasson I, Mesnard JM, et al. (2009) Upregulation of human T-cell leukemia virus type 1 antisense transcription by the viral tax protein. J Virol 83: 2048–2054.
20. Gaudray G, Gachon F, Basbous J, Biard-Piechaczyk M, Devaux C, et al. (2002) The complementary strand of the human T-cell leukemia virus type 1 RNA genome encodes a bZIP transcription factor that down-regulates viral transcription. J Virol 76: 12813–12822.
21. Ciuffi A, Llano M, Poeschla E, Hoffmann C, Leipzig J, et al. (2005) A role for LEDGF/p75 in targeting HIV DNA integration. Nat Med 11: 1287–1289.
22. Bernstein BE, Birney E, Dunham I, Green ED, Gunter C, et al. (2012) An integrated encyclopedia of DNA elements in the human genome. Nature 489: 57–74.
23. Durand CM, Blankson JN, Siliciano RF (2012) Developing strategies for HIV-1 eradication. Trends Immunol 33: 554–562.
24. Bangham CR, Meekings K, Toulza F, Nejmeddine M, Majorovits E, et al. (2009) The immune control of HTLV-1 infection: selection forces and dynamics. Front Biosci 14: 2889–2903.
25. Tattermusch S, Skinner JA, Chaussabel D, Banchereau J, Berry MP, et al. (2012) Systems biology approaches reveal a specific interferon-inducible signature in HTLV-1 associated myelopathy. PLoS Pathog 8: e1002480.
26. Santoni FA, Hartley O, Luban J (2010) Deciphering the code for retroviral integration target site selection. PLoS Comput Biol 6: e1001008.
27. Rain JC, Cribier A, Gerard A, Emiliani S, Benarous R (2009) Yeast two-hybrid detection of integrase-host factor interactions. Methods 47: 291–297.
28. Cherepanov P, Maertens G, Proost P, Devreese B, Van Beeumen J, et al. (2003) HIV-1 integrase forms stable tetramers and associates with LEDGF/p75 protein in human cells. J Biol Chem 278: 372–381.
29. Maertens G, Cherepanov P, Pluymers W, Busschots K, De Clercq E, et al. (2003) LEDGF/p75 is essential for nuclear and chromosomal targeting of HIV-1 integrase in human cells. J Biol Chem 278: 33528–33539.
30. Shan L, Yang HC, Rabi SA, Bravo HC, Shroff NS, et al. (2011) Influence of host gene transcription level and orientation on HIV-1 latency in a primary-cell model. J Virol 85: 5384–5393.
31. Euskirchen G, Auerbach RK, Snyder M (2012) SWI/SNF Chromatin-remodeling Factors: Multiscale Analyses and Diverse Functions. J Biol Chem 287: 30897–30905.
32. Ho L, Jothi R, Ronan JL, Cui K, Zhao K, et al. (2009) An embryonic stem cell chromatin remodeling complex, esBAF, is an essential component of the core pluripotency transcriptional network. Proc Natl Acad Sci U S A 106: 5187–5191.
33. De S, Wurster AL, Precht P, Wood WH, 3rd, Becker KG, et al. (2011) Dynamic BRG1 recruitment during T helper differentiation and activation reveals distal regulatory elements. Mol Cell Biol 31: 1512–1527.
34. Euskirchen GM, Auerbach RK, Davidov E, Gianoulis TA, Zhong G, et al. (2011) Diverse roles and interactions of the SWI/SNF chromatin remodeling complex revealed using global approaches. PLoS Genet 7: e1002008.
35. Easley R, Carpio L, Guendel I, Klase Z, Choi S, et al. (2010) Human T-lymphotropic virus type 1 transcription and chromatin-remodeling complexes. J Virol 84: 4755–4768.
36. Rafati H, Parra M, Hakre S, Moshkin Y, Verdin E, et al. (2011) Repressive LTR nucleosome positioning by the BAF complex is required for HIV latency. PLoS Biol 9: e1001206.
37. Kalpana GV, Marmon S, Wang W, Crabtree GR, Goff SP (1994) Binding and stimulation of HIV-1 integrase by a human homolog of yeast transcription factor SNF5. Science 266: 2002–2006.
38. Turelli P, Doucas V, Craig E, Mangeat B, Klages N, et al. (2001) Cytoplasmic recruitment of INI1 and PML on incoming HIV preintegration complexes: interference with early steps of viral replication. Mol Cell 7: 1245–1254.
39. Matsuoka M, Jeang KT (2011) Human T-cell leukemia virus type 1 (HTLV-1) and leukemic transformation: viral infectivity, Tax, HBZ and therapy. Oncogene 30: 1379–1389.
40. Marriott SJ, Semmes OJ (2005) Impact of HTLV-I Tax on cell cycle progression and the cellular DNA damage repair response. Oncogene 24: 5986–5995.
41. Asquith B, Zhang Y, Mosley AJ, de Lara CM, Wallace DL, et al. (2007) In vivo T lymphocyte dynamics in humans and the impact of human T-lymphotropic virus 1 infection. Proc Natl Acad Sci U S A 104: 8035–8040.
42. Kannagi M, Harada S, Maruyama I, Inoko H, Igarashi H, et al. (1991) Predominant recognition of human T cell leukemia virus type I (HTLV-I) pX gene products by human CD8+ cytotoxic T cells directed against HTLV-I-infected cells. Int Immunol 3: 761–767.
43. Taniguchi Y, Nosaka K, Yasunaga J, Maeda M, Mueller N, et al. (2005) Silencing of human T-cell leukemia virus type I gene transcription by epigenetic mechanisms. Retrovirology 2: 64.
44. Kattan T, MacNamara A, Rowan AG, Nose H, Mosley AJ, et al. (2009) The avidity and lytic efficiency of the CTL response to HTLV-1. J Immunol 182: 5723–5729.
45. Nejmeddine M, Barnard AL, Tanaka Y, Taylor GP, Bangham CR (2005) Human T-lymphotropic virus, type 1, tax protein triggers microtubule reorientation in the virological synapse. J Biol Chem 280: 29653–29660.
46. Nejmeddine M, Negi VS, Mukherjee S, Tanaka Y, Orth K, et al. (2009) HTLV-1-Tax and ICAM-1 act on T-cell signal pathways to polarize the microtubule-organizing center at the virological synapse. Blood 114: 1016–1025.
47. Niewiesk S, Daenke S, Parker CE, Taylor G, Weber J, et al. (1995) Naturally occurring variants of human T-cell leukemia virus type I Tax protein impair its recognition by cytotoxic T lymphocytes and the transactivation function of Tax. J Virol 69: 2649–2653.
48. Richardson JH, Edwards AJ, Cruickshank JK, Rudge P, Dalgleish AG (1990) In vivo cellular tropism of human T-cell leukemia virus type 1. J Virol 64: 5682–5687.
49. Hanon E, Stinchcombe JC, Saito M, Asquith BE, Taylor GP, et al. (2000) Fratricide among CD8(+) T lymphocytes naturally infected with human T cell lymphotropic virus type I. Immunity 13: 657–664.
50. Asquith B, Mosley AJ, Heaps A, Tanaka Y, Taylor GP, et al. (2005) Quantification of the virus-host interaction in human T lymphotropic virus I infection. Retrovirology 2: 75.
51. Miyoshi I, Kubonishi I, Sumida M, Hiraki S, Tsubota T, et al. (1980) A novel T-cell line derived from adult T-cell leukemia. Gann 71: 155–156.
52. Giardine B, Riemer C, Hardison RC, Burhans R, Elnitski L, et al. (2005) Galaxy: a platform for interactive large-scale genome analysis. Genome Res 15: 1451–1455.
53. Goecks J, Nekrutenko A, Taylor J (2010) Galaxy: a comprehensive approach for supporting accessible, reproducible, and transparent computational research in the life sciences. Genome Biol 11: R86.
54. Blankenberg D, Von Kuster G, Coraor N, Ananda G, Lazarus R, et al. (2010) Galaxy: a web-based genome analysis tool for experimentalists. Curr Protoc Mol Biol Chapter 19: Unit 19 10 11–21.
55. Nagai M, Usuku K, Matsumoto W, Kodama D, Takenouchi N, et al. (1998) Analysis of HTLV-I proviral load in 202 HAM/TSP patients and 243 asymptomatic HTLV-I carriers: high proviral load strongly predisposes to HAM/TSP. J Neurovirol 4: 586–593.
56. Karolchik D, Hinrichs AS, Furey TS, Roskin KM, Sugnet CW, et al. (2004) The UCSC Table Browser data retrieval tool. Nucleic Acids Res 32: D493–496.
57. Jothi R, Cuddapah S, Barski A, Cui K, Zhao K (2008) Genome-wide identification of in vivo protein-DNA binding sites from ChIP-Seq data. Nucleic Acids Res 36: 5221–5231.

ELSEVIER

Institut Pasteur

Microbes and Infection 15 (2013) 491–505

www.elsevier.com/locate/micinf

Original article

Viral interference with host mRNA surveillance, the nonsense-mediated mRNA decay (NMD) pathway, through a new function of HTLV-1 Rex: implications for retroviral replication

Kazumi Nakano [a], Tomomi Ando [a,b], Makoto Yamagishi [a], Koichi Yokoyama [a], Takaomi Ishida [c], Takeo Ohsugi [d], Yuetsu Tanaka [e], David W. Brighty [f], Toshiki Watanabe [a,*]

[a] *Laboratory of Tumor Cell Biology, Department of Medical Genome Sciences, Graduate School of Frontier Sciences, The University of Tokyo, 4-6-1, Shirokanedai, Minatoku, Tokyo 108-8639, Japan*

[b] *Department of Virology II, National Institute of Infectious Diseases, 1-23-1, Toyama, Shinjukuku, Tokyo 162-8640, Japan*

[c] *Research Center for Asian Infectious Diseases, The Institute of Medical Science, The University of Tokyo, 4-6-1, Shirokanedai, Minatoku, Tokyo 108-8639, Japan*

[d] *Center for Animal Resources and Development, The University of Kumamoto, 2-2-1, Honsho, Kumamoto 860-0811, Japan*

[e] *Department of Immunology, Graduate School of Medicine, University of the Ryukyus, 207 Uehara, Nishihara-cho, Nakagusuku, Okinawa 903-0215, Japan*

[f] *Division of Cancer Research, Medical Research Institute, University of Dundee, Scotland DD1 9SY, UK*

Received 9 January 2013; accepted 18 March 2013
Available online 27 March 2013

Abstract

Nonsense-mediated mRNA decay (NMD) is an essential and conserved cellular mRNA quality control mechanism. RNA signals to express viral genes from overlapping open reading frames potentially initiate NMD, nevertheless it is not clear whether viral RNAs are sensitive to NMD or if viruses have evolved mechanisms to evade NMD. Here we demonstrate that the genomic and full-length mRNAs of Human-T-cell Leukemia Virus type-I (HTLV-1), a retrovirus responsible for Adult T-cell Leukemia (ATL), are sensitive to NMD. They exhibit accelerated turnover in NMD-activated cells, while siRNA-mediated knockdown of NMD-master-regulator, UPF1, promotes enhanced stability of them. These effects on RNA stability were recapitulated by a reporter construct encoding the HTLV-1 translational frameshift signal of *gag-pol*. In agreement with the RNA stability, viral protein expression from the integrated provirus was inversely correlated with cellular NMD activity. We further demonstrated that the viral RNA-binding protein, Rex, approves the stability of viral RNA by inhibiting NMD. Significantly, Rex establishes a general block to NMD, as both NMD-responsive reporter transcripts and natural host-encoded NMD substrates were stabilized in the presence of Rex. Thus, we suggest that Rex not only stabilizes viral transcripts, but also perturbs cellular mRNA metabolism and host cell homeostasis via inhibition of NMD.
© 2013 Institut Pasteur. Published by Elsevier Masson SAS. All rights reserved.

Keywords: HTLV-1; HTLV-1 Rex; NMD; Retroviral genomic RNA; Host–pathogen interaction

1. Introduction

Nonsense-mediated mRNA decay (NMD) is an mRNA surveillance mechanism that is conserved in eukaryotic cells. The degradation of aberrant mRNAs containing premature termination codons (PTCs) is the most studied NMD function. Positioned upstream of the natural end of open reading frames (ORFs), PTCs are stop codons that arise from frameshifts due to mutations or aberrant mRNA processing events. Truncated proteins encoded by such abnormal mRNAs are often deleterious to cells because they may be structurally unstable and result in translation product aggregation or may function as dominant negative inhibitors of wild-type (WT) protein function [1]. Recently, it has been recognized that NMD function is important for eliminating aberrant mRNAs and

* Corresponding author. Tel.: +81 3 5449 5298; fax: +81 3 5449 5418.
E-mail addresses: tnabe@ims.u-tokyo.ac.jp, tnabe@k.u-tokyo.ac.jp (T. Watanabe).

1286-4579/$ - see front matter © 2013 Institut Pasteur. Published by Elsevier Masson SAS. All rights reserved.
http://dx.doi.org/10.1016/j.micinf.2013.03.006

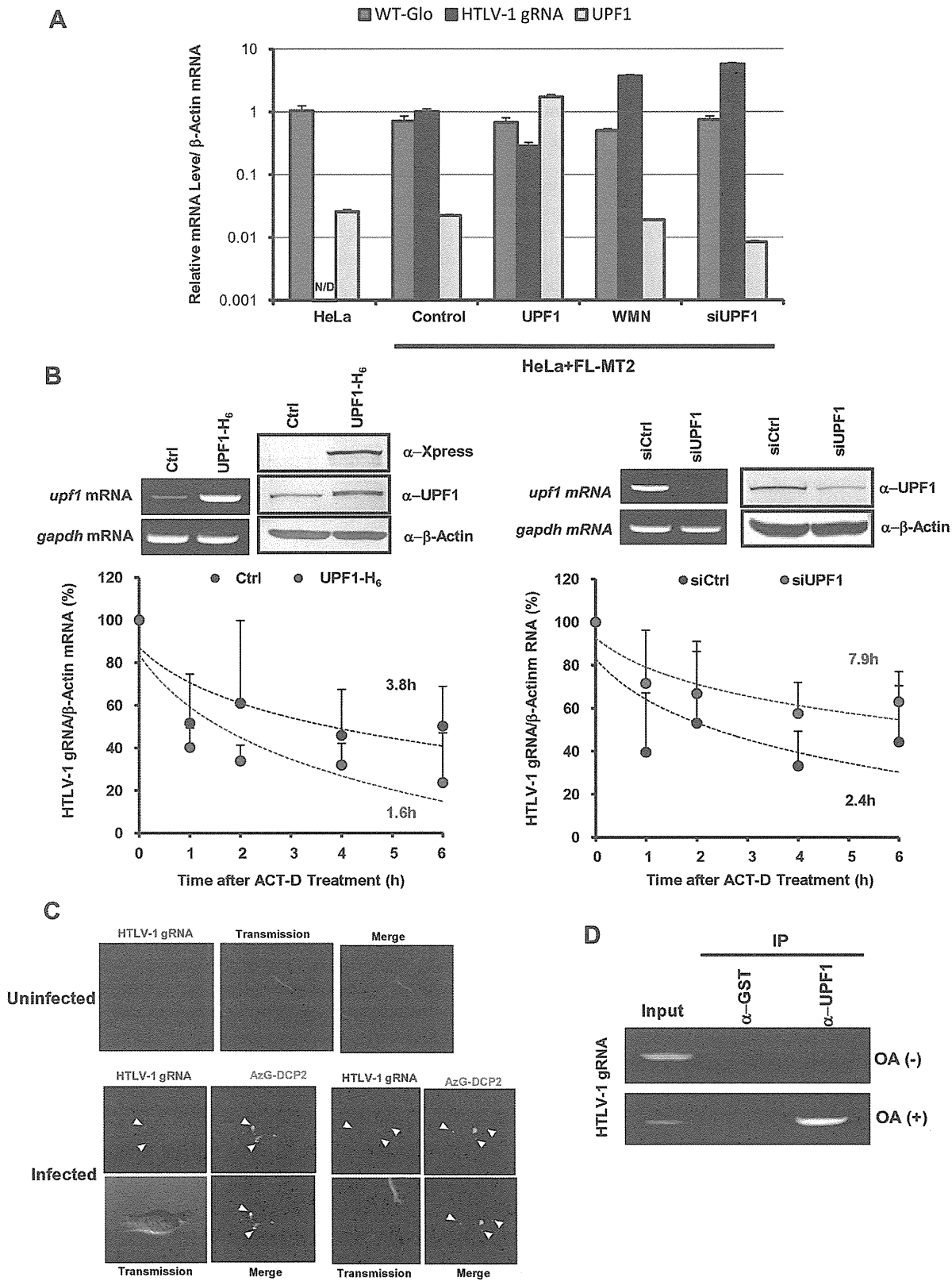

Fig. 1. HTLV-1 genomic unspliced RNA is a NMD target. (A) Changes in the cellular level of HTLV-1 unspliced mRNA were dependent on cellular NMD activity. The steady-state level of HTLV-1 genomic primary transcripts (HTLV-1 gRNA) accumulating from the pFL-MT2 infectious clone in HeLa cells was decreased by UPF1 overexpression and increased by NMD inhibition through siUPF1 transfection or wortmannin treatment. By contrast, the level of WT-β-globin mRNA (WT-Glo), which is not a NMD target, was not influenced by the cellular level of UPF1 or wortmannin treatment, indicating that the level of HTLV-1 genomic mRNA is selectively influenced by cellular NMD activity. (B) UPF1-dependent HTLV-1 genomic mRNA instability in HTLV-1 infected HeLa cells by co-cultivation with

controlling the expression levels of a considerable number of normal cellular mRNAs that possess NMD-activating structures, such as uORFs and introns within the 3′ untranslated region (UTR) [2]. The NMD machinery achieves these functions by coupling with the splicing and translational machinery [3,4]. Thus, NMD is an essential mechanism that governs mRNA quality and quantity in eukaryotic cells.

RNA viruses have compact genomes, but they have evolved elegant mechanisms to maximize coding potential and precisely regulate the expression of encoded genes. Overlapping reading frames, internal ribosome entry sites, alternative splicing, suboptimal Kozak sequences, and ribosomal frameshifting are among the varied mechanisms used to maximize genomic coding potential and regulate viral gene expression [5]. The presence of such signals in cellular mRNA is unusual, but wherever they occur, there is significant potential to activate the NMD pathway, which destabilizes RNA and increases mRNA turnover [6–8]. Programmed Ribosomal Frameshift (PRF) is a mechanism frequently used by viruses to alter the translational reading frame by shifting the ribosome at a frameshifting sequence often referred to as a "slippery site" [9]. Especially, *pgk1* mRNA stability assays with or without L-A viral −PRF signal showed that −PRF itself functioned as *cis*-acting destabilization element through NMD [7]. In addition, as many as one-third of all cellular mRNA variants produced by alternative splicing are reported to be potential targets of NMD [6,8]. As reviewed by Dickson and Wilusz [10], virus–host mRNA surveillance interface is attracting growing interest as a new aspect of host–pathogen interactions. Nevertheless, viral mechanisms to evade host mRNA surveillance to protect its own RNA has been mostly left uninvestigated. Accumulated knowledge indicates that viruses have various strategies to avoid or incapacitate host mRNA decay. Therefore, for RNA viruses, there are important unresolved questions. First, are RNA viruses that possess overlapping reading frames, alternative stop codons, and translational frameshift sequences sensitive to NMD? If so, do RNA viruses actively avoid the NMD surveillance pathway? Finally, are viral factors required for evasion of host-encoded NMD?

The human T-cell leukemia virus type I (HTLV-1) is a delta retrovirus that causes aggressive adult T-cell leukemia (ATL) in some infected individuals. The genomic RNA of this retrovirus encodes more than ten ORFs with associated stop codons within a full-length genomic RNA of 8685 nucleotides. HTLV-1 employs a number of mechanisms to achieve appropriate and ordered expression of these genes, including alternative splicing and PRF. In particular, Gag, Pro, and Pol, is translationally regulated by in-frame read-through and two −1 PRF signals at 1718 and 2245 nucleotides, respectively. In addition, the HTLV-1 genomic RNA contains two major splice sites. Unspliced HTLV-1 RNA yields Gag, Pro, and Pol proteins, singly spliced RNA produces Env, while the functional proteins derived from the pX region can be translated only from double-spliced mRNA. Therefore, we hypothesized that because of the unusual structure and processing signals, which include multiple stop codons, translational frameshifts, and a downstream splice acceptor site, the full-length HTLV-1 genomic RNA and *gag/pol* mRNA appear to be prime candidates for interference with viral mRNA accumulation via NMD.

Here we explored whether the presence of multiple stop codons and −1 PRF signals in HTLV-1 viral transcripts activates the host NMD. Also, we investigated how such viral RNA survives in the face of a highly efficient cellular mRNA quality control system.

2. Materials and methods

2.1. NMD reporter constructs and assays

To measure overall cellular NMD activity, we constructed NMD reporter plasmids based on widely used β-globin as well as on a HTLV-1 *gag* mRNA fragment. The β-globin-based NMD reporter plasmid was created based on Boelz et al. [11] with modification dependent on the type of experiment. Detailed methods of reporter construction and luciferase assays are available in Supplementary material.

2.2. HTLV-1 expression in HeLa cells

To express HTLV-1 in HeLa cells, transfection of an infectious clone (pFL-MT2) [12] (for Fig. 1A) or co-cultivation with MT-2 (for Fig. 1B–D, 3C–E, 6B–D) was employed. Please see Supplementary material for more detail.

2.3. Inhibition of UPF1 and UPF2

The siRNA sequences against *upf1* mRNA and *upf2* mRNA are described elsewhere [13,14]. The sequence of the control siRNA was 5′-AGGUCGAACUACGGGUCAA(TT)-3′. Wortmannin is a PI3K inhibitor and known to inhibit UPF1 activity by inhibiting SMG1, the kinase of UPF1. For complete inhibition of UPF1 activity, cells were treated with 100 μM wortmannin for 19–20 h before sampling. For construction of

MT-2 cells. The stability of HTLV-1 genomic mRNA decreased in the cells overexpressing His-tagged UPF1 (UPF1-H_6) (half-life = 1.6 h) compared with control (Ctrl) cells transfected with the empty vector (half-life = 3.8 h). In contrast, the stability of HTLV-1 genomic mRNA in cells transfected with siUPF1 (half-life = 7.9 h) increased compared with that in cells transfected with the control siRNA (siCtrl) (half-life = 2.4 h). The half-life was calculated based on the regression curve (dashed line). Above each graph, semi-quantitative RT-PCR analysis of relative RNA levels (left panel) and Western blotting analysis of protein levels (right panel) are shown ($n = 4$, mean ± SE). (C) HTLV-1 genomic RNA, detected by in situ hybridization with the *gag/pol* cDNA probe in HTLV-1 infected HeLa cells, co-localized with AzamiGreen-DCP2, a P-body marker, indicating that a notable fraction of HTLV-1 genomic unspliced RNA (gRNA) accumulates in P-bodies. No clear signals in negative control HeLa cells without infection confirmed that the *gag/pol* cDNA probe specifically detected gRNA in infected HeLa cells. (D) Interaction between UPF1 and HTLV-1 unspliced mRNA. HTLV-1 genomic unspliced mRNA was found in the UPF1 complex co-immunoprecipitated with anti-UPF1 antibody from whole-cell lysate of MT-2 cells (top panel). Moreover, sustained phosphorylation of UPF1 through okadaic acid (OA) treatment increased the level of bound HTLV-1 genomic mRNA recovered (bottom panel).

an antisense (As)-*upf2* mRNA-expressing plasmid and suppression of UPF2, please see Supplementary material.

2.4. Measurement of mRNA stability

First, the cells (3×10^5/mL) were resuspended in culture medium, and 1.5×10^5/500 μL of the cells were sampled as the 0 h sample. Second, the culture medium was replaced by that containing actinomycin D (5 μg/mL) and seeded at 1.5×10^5/500 μL in 5 wells of a 12-well plate. The cells were sampled 1, 2, 3, 4, and/or 6 h after the addition of actinomycin D to each well, and total RNA was extracted using Isogen (Nippon Gene Co., Ltd.) for the measurement of mRNA levels by real-time PCR. The levels of NMD target mRNAs (MAP3K14, IL6, DUSP10, Fyn, PTPRF, ARHGEF18, ASNS, and DEXI) were measured at each time point and standardized by the corresponding β-actin mRNA level, which is not a NMD target. Methods in establishment of CEM cells, which stably overexpress Rex protein are available in Supplementary material.

2.5. Protein expression plasmids

The UPF1 expression plasmid was constructed by inserting the full-length cDNA fragment of human *upf1* into the *Eco*RI site of pCDNA3.1/His C (Invitrogen) for His/Xpress-UPF1 expression. The expression plasmids of HTLV-1 regulatory proteins were constructed by inserting the PCR-amplified cDNA fragments of HTLV-1 *rex*, *tax*, *p30ii*, *p12*, *p13*, and *hbz* from a cDNA pool derived from MT-2 cells at the *Xho*I/*Spe*I sites of pME-FLAG for FLAG-tagged proteins. The *dcp2* cDNA fragment was inserted at the *Bam*HI site of pmAG1-MN1 (Amalgaam Co., Ltd.) for AzamiGreen-tagged DCP2 expression.

2.6. Quantitative and semi-quantitative RT-PCR and genomic DNA PCR

The levels of viral and host cell transcripts were measured by quantitative or semi-quantitative RT-PCR. Total RNA was extracted using Isogen (Nippon Gene Co., Ltd.) following the manufacturer's protocol. DNase I treatment was performed to eliminate genomic DNA contamination. Extracted total RNA samples were subjected to reverse transcription using SuperScript II (Invitrogen), followed by quantitative real-time PCR using SYBR Premix Ex Taq (Takara Bio Inc.) and thermal cycler dice (Takara) or by semi-quantitative PCR. The sequences of primers used for PCR are available in Supplementary material.

2.7. Western blotting and antibodies

For the Western blotting of HTLV-1 Tax, a monoclonal Tax antibody (LT-4) was used [15]. Rex antibody, used in Western blotting for the HTLV-1 Rex protein, was monoclonal rat antiserum (Tanaka, unpublished data), while HTLV-1 Gag-p19 and Gag-p24 antibodies were the monoclonal mouse antibodies, GIN-7 and NOR-1, respectively [16]. The following primary antibodies were purchased from the indicated companies: hUPF1 (#9435; Cell Signaling Technology Inc.), hUPF2 (ab28712-200; Abcam), FLAG (F3165; Sigma–Aldrich Corporation), GST (#27-4577-01; GE Healthcare Bioscience), Xpress (46-0528; Invitrogen), β-actin (sc-69879; Santa Cruz Biotechnology, Inc.). For the secondary antibodies conjugated with alkaline phosphatase, anti-mouse IgG (S372B; Promega), anti-rabbit IgG (S373B; Promega), or anti-goat IgG (V115A; Promega) was used depending on the host species of the primary antibody.

2.8. Indirect immunofluorescence in situ RNA hybridization assays

HeLa cells transiently expressing AzamiGreen-DCP2 was co-cultured with MT-2 at 37 °C for 24 h to express HTLV-1. MT-2 cells were removed by washing 3 times with PBS, then the infected HeLa cells were further incubated at 37 °C for 24 h. In situ hybridization of HTLV-1 unspliced mRNA was performed by incubating the fixed and permeabilized cells with DIG-labeled HTLV-1 *gag/pol* cDNA probes at 37 °C for 16 h. The hybridized probes were detected by immunocytochemistry using rhodamine-conjugated anti-DIG antibody (Roche). The subcellular localization of HTLV-1 unspliced mRNA and AzamiGreen-DCP2 was observed using a confocal laser scanning microscope (LSM510; Carl Zeiss AG). As negative control, HeLa cells without HTLV-1 infection were also subjected to the same hybridization procedure.

2.9. RNA immunoprecipitation (RIP) assay

RIP assay between UPF1 and HTLV-1 genomic unspliced mRNA was performed following a method described elsewhere [17]. UFP1 was co-immunoprecipitated from the whole cell lysate of MT-2 using goat polyclonal antibody against hUPF1 (Rent-1 (p-14), sc-18260; Santa Cruz Biotechnology, Inc.), and total RNA was extracted from the immunoprecipitant for detection of HTLV-1 genomic unspliced RNA (gRNA) by RT-PCR using primers for the HTLV-1 *gag* region. Immunoprecipitation by a goat polyclonal antibody against GST (GE Healthcare Bioscience) was performed as a negative control. Total RNA from the whole cell lysate (22% vol. of input to immunoprecipitation) was also extracted for RT-PCR of gRNA.

2.10. Statistical analyses

Throughout the present study, two-tailed paired Student's *t*-test was performed to test the statistical difference between the experimental groups. Asterisks in the figures indicate a significant difference between the tested groups ($*p < 0.05$; $**p < 0.01$; and $***p < 0.001$, $n > 3$).

3. Results

3.1. The cellular UPF1 level influences the turnover rate of HTLV-1 unspliced mRNA

To test the hypothesis that NMD inhibits or antagonizes HTLV-1 replication, the accumulation of genomic primary

mRNA was examined in human HeLa cells transfected with an infectious HTLV-1 molecular clone, pFL-MT2 [12], in the presence of the overexpressed key NMD-positive effector, UPF1, or following siRNA-mediated knockdown of UPF1 (Fig. 1A). In the presence of ectopic UPF1, the steady-state level of HTLV-1 genomic unspliced mRNA (gRNA) accumulating from the pFL-MT2 infectious clone significantly decreased, whereas it increased following NMD inhibition by wortmannin treatment or following knockdown with UPF1-specific siRNAs (Fig. 1A). The level of WT-β-globin mRNA, which is not a NMD target, was not significantly influenced by the cellular level of UPF1 or by wortmannin treatment, indicating that the level of HTLV-1 genomic RNA was selectively influenced by cellular NMD activity (Fig. 1A). Reverse-transcriptase (−) PCR with *gag* primers was conducted in all above cDNA samples and it was confirmed that no detectable level of genomic DNA was contaminated in these samples (data not shown). In addition, the viral genomic unspliced RNA was significantly destabilized following UPF1 overexpression in infected cells (half-life = 1.6 h) compared with control cells with endogenous levels of UPF1 (half-life = 3.8 h) (Fig. 1B, left panel). In stark contrast, HTLV-1 unspliced RNA was stabilized after UPF1 knockdown by siUPF1 in infected cells (half-life = 7.9 h) compared to the control cells transfected with the control siRNA (half-life = 2.4 h) (Fig. 1B right panel). In cells, the factors required for NMD activity are often associated with cytoplasmic foci known as processing bodies (P-bodies). Therefore, the subcellular localization of HTLV-1 genomic unspliced RNA was examined in HTLV-1 infected HeLa cells by in situ hybridization and compared with the distribution of Azami-Green labeled de-capping protein 2 (DCP2) protein, which is a known P-body marker. HTLV-1 unspliced RNA (gRNA) was observed throughout the cytoplasm, but a substantial fraction of the RNA co-localized with DCP2 in brightly stained granular centers, suggesting that a significant level of the viral RNA localized to the P-bodies (Fig. 1C). Moreover, immunoprecipitation assays demonstrated that UPF1 is in a complex with HTLV-1 unspliced RNA and the amount of viral RNA interacting with UPF1 depends on the phosphorylation status of UPF1, i.e., phosphorylated UPF1 with okadaic acid treatment interacted with a higher amount of HTLV-1 genomic unspliced RNA (Fig. 1D). These data support the notion that HTLV-1 unspliced RNA is specifically targeted by UPF1 for processing via the NMD pathway.

3.2. HTLV-1 derived reporter activity is NMD sensitive

To further examine the impact of NMD on HTLV-1 RNA stability, a luciferase-based reporter plasmid was constructed (Fig. 2A). The reporter comprises the renilla luciferase ORF fused in-frame with the 5′ end of a HTLV-1 fragment spanning the 3′ end of *gag* through *pro* and into the 5′ end of *pol* (1677–2594 nt). The HTLV-1 sequences are followed at the 3′ end by a β-globin splicing sequence, which is positioned for recruitment of the exon junction complex (EJC) downstream of the HTLV-1 frameshift fragment. Splicing at the correct site, i.e., between exon 2 and exon 3 of β-globin mRNA, has been confirmed by sequencing PCR-amplified transcripts produced from the reporter (data not shown). This reporter provides four possible translation patterns, of which three generate a PTC and are expected to trigger NMD (Fig. 2A). The impact of siRNA knockdown of UPF1 or UPF2, which led to the suppression of NMD activity, on HTLV-1 derived reporter activity was examined in HeLa cells. Of note, the reporter activities increased in HeLa cells treated with siUPF1 and siUPF2 (Fig. 2B). Thus, reporter transcripts spanning 1677–2594 nucleotides of HTLV-1 genomic RNA are stabilized by NMD inhibition and are consequently targeted by NMD.

3.3. NMD activity in HTLV1 transformed cell lines

To determine cellular NMD activity, we employed a luciferase-based β-globin reporter system, which encodes renilla luciferase that is linked to the WT β-globin gene sequence as a control (WT-Glo) or an essentially identical construct but with a PTC-harboring β-globin gene sequence downstream of renilla ORF (PTC-Glo) (Fig. 3A). This β-globin-based reporter provides a robust and reliable readout of cellular NMD activity in HeLa cells (Fig. 3A) and in the T-cell line, Jurkat (Fig. S1).

To determine if cell transformation by HTLV-1 specifically perturbs NMD activity, we tested NMD activity in control HTLV-1-unrelated cell lines (fibroblasts and T cell lines) and in HTLV-1 infected T cell lines. In these assays, the control HTLV-1-unrelated cell lines showed relative NMD activities of >80% of that in control HeLa cells, which have intact NMD activity. In contrast, the NMD values for HTLV-1 infected (i.e., HTLV-1-transformed and ATL-derived) T cell lines were <50% of that observed in control HeLa cells, indicating lower NMD activities (Fig. 3B). These results raised the possibility that NMD is partially suppressed or inhibited in HTLV-1 infected cells and in ATL cells.

3.4. Impact of HTLV-1 infection on NMD activity

To examine whether HTLV-1 infection has any effect on the host cell NMD activity, sHeLa cells, which stably express both firefly-PTC-Glo and renilla-WT-Glo reporter genes, were infected with HTLV-1 by co-cultivation with MT-2 cells. Successful infection of HTLV-1 from MT-2 to sHeLa cells was confirmed by detection of HTLV-1 unspliced mRNAs by semi-quantitative RT-PCR (Fig. 3C). The expression of HTLV-1 unspliced mRNA was evaluated 1–4 days after infection. The highest levels of unspliced RNA were observed during the first 2 days of infection, corresponding to the peak levels of HTLV-1 *tax/rex* mRNAs and the Tax and Rex proteins (Fig. 3C). To confirm successful infection in HeLa cells co-cultured with MT-2, the expression pattern of the Tax protein was observed by immunocytochemistry (Fig. S2A). Genomic fingerprinting PCR of the human MCT118 locus in the infected sHeLa cells showed no MT-2-derived bands, confirming that viral proteins detected in the infected sHeLa cells were attributed to HTLV-1

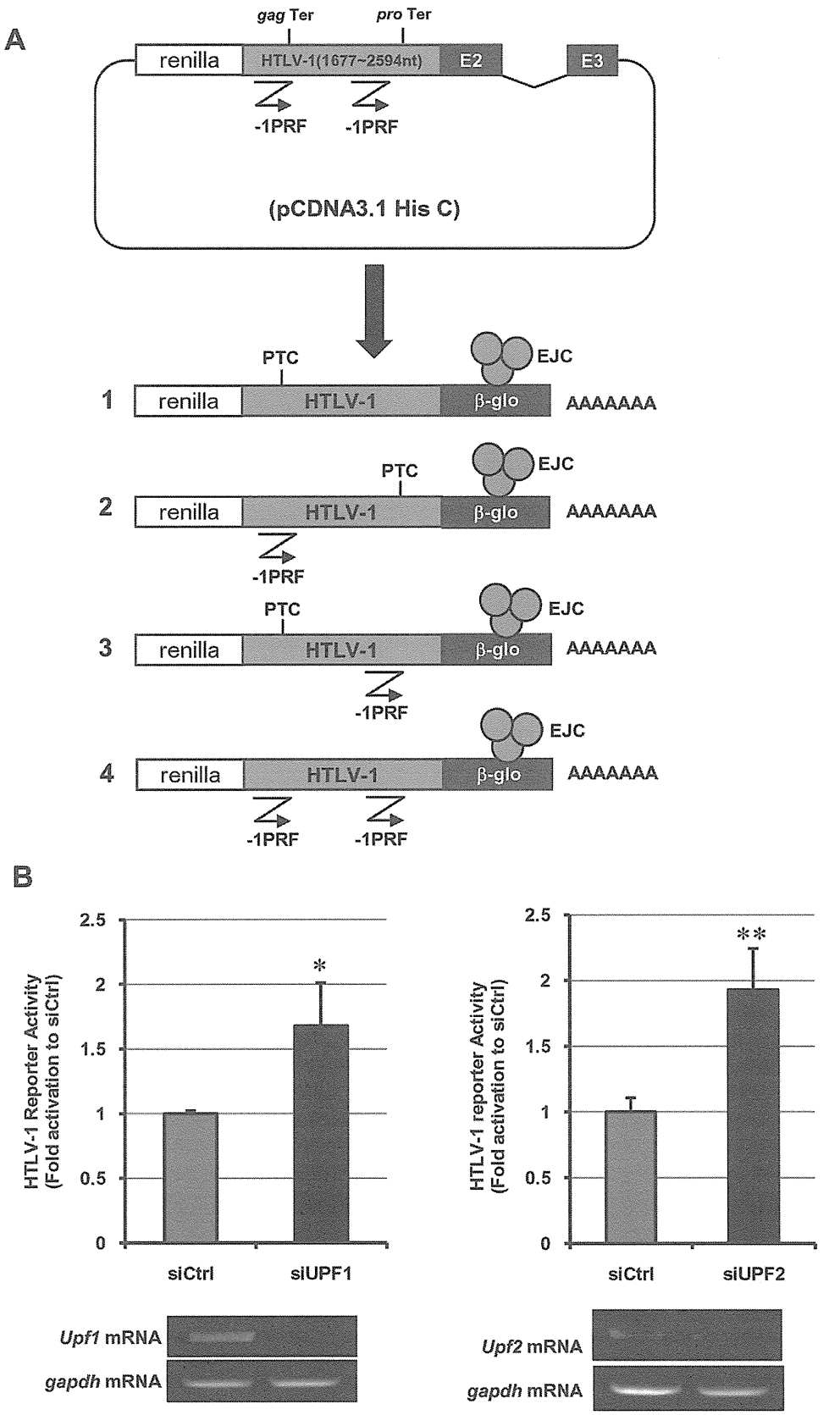

Fig. 2. HTLV-1 derived reporter activity is NMD sensitive. (A) A schematic structure of the HTLV-1 derived reporter plasmid and four possible translation patterns. As indicated, the HTLV-1 fragment in the reporter plasmid contains two −1 PRF signals (shown by ↯) and 3/4 of these translation patterns result in PTC. (B) The HTLV-1 derived reporter activity was NMD dependent in HeLa cells. The relative HTLV-1 reporter activity was increased by NMD inhibition through siRNA-mediated suppression of UPF1 and UPF2 ($n = 3–5$, mean ± SD; *$p < 0.05$; **$p < 0.01$).

infection but not to contamination of co-cultured MT-2 cells (for genomic fingerprinting PCR, see Supplementary material and methods for more details) (Fig. S2B). NMD activity in these HTLV-I-infected sHeLa cells was significantly suppressed on day 1 ($p < 0.05$) and on day 2 ($p < 0.01$) after infection compared with that in control sHeLa cells co-cultured with uninfected cells (Fig. 3D). These results indicated that HTLV-1 caused a temporal suppression of NMD activity. Of note, the timing of maximum suppression of NMD activity corresponded to the peak expression of HTLV-1 *tax/rex* mRNAs and proteins and correlated with peak accumulation of HTLV-1 unspliced mRNA (Fig. 3C and D). Moreover, co-culture of sHeLa cells with MT-2 in the presence of the reverse transcriptase inhibitor azidothymidine (AZT) resulted in a dose-dependent rescue of NMD activity, supporting the idea that the suppression of NMD activity is indeed caused by HTLV-1 infection of target sHeLa cells and that this suppression requires reverse transcription and provirus integration (Fig. 3E).

3.5. HTLV-1 Rex is the principal viral factor inhibiting host NMD activity

Next, we examined HTLV-1 gene products for the ability to suppress host NMD activity. The relative NMD activity in sHeLa cells that ectopically express p27Rex (Rex), p21Rex, p30II, and Tax was analyzed using the dual-luciferase NMD reporter assay at 24,36, and 48 h after transfection. As shown in Fig. 4A, NMD activity was significantly suppressed 24 h after transfection when p27Rex or p21Rex was expressed. In these experiments, the HTLV-1 transcriptional transactivator Tax was also found to inhibit NMD activity, but this effect was consistently less than that observed for p27Rex or p21Rex.

The most significant impact on host NMD activity was the dose-dependent suppression exerted by p27Rex and to a slightly lesser degree, p21Rex (Fig. 4B). Of note, NMD reporter constructs do not contain sequences corresponding to the highly structured RxRE. Consequently, we suggest that the suppression of NMD activity by Rex is not due to RxRE-dependent and Rex-mediated nuclear export of unspliced mRNAs. Indeed, nuclear export of unspliced β-globin mRNA, transcribed from the reporter plasmid, was not enhanced by Rex (Fig. S3A). We also confirmed that insertion of RxRE after the β-globin sequence of the NMD reporter plasmid did not exhibit any significant influence on Rex-induced NMD inhibition (Fig. S3B). Moreover, our study demonstrated that p21Rex, which lacks the N-terminal RxRE-binding domain, also exhibited NMD inhibitory activity, supporting the view that NMD inhibition is due to a genetically separable aspect of Rex function that is independent of the arginine-rich RxRE-binding motif. Other HTLV-1 accessory proteins, such as p12, p13, and antisense-encoded HBZ, did not show any significant influence on the cellular NMD activity (Fig. S4).

3.6. Rex inhibits global NMD activity of the cell

On confirmation that Rex stabilizes chimeric NMD reporter mRNA, we tested if Rex stabilizes endogenous NMD target mRNA. Fig. 5 shows the decay rates of NMD target mRNAs in CEM cells stably expressing Rex or in control cells showing no Rex expression. The selected mRNAs contained uORFs (MAP3K14, IL6, DUSP10, Fyn, PTPRF, ARHGEF18, and ASNS) or 3′ UTR intron (DEXI) as NMD-inducing features and stabilization under UPF1 knockdown was confirmed (MAP3K14, PTPRF, ARHGEF18, and ASNS) or expected (DUSP10, Fyn, IL6, and DEXI) by Mendell et al. [2]. The graphs show that these mRNA substrates for NMD are significantly stabilized by Rex overexpression in a T cell line. These NMD target mRNAs were specifically stabilized in CEM-Rex, since the stability of β-actin mRNA, a non-NMD target, was almost the same between CEM-empty and CEM-Rex when the stabilities of β-actin mRNA and NMD target mRNA were separately illustrated (data not shown). These results provide strong evidence that Rex serves as a general inhibitor of NMD.

3.7. NMD inhibition by Rex enhances HTLV-1 expression

Finally, we examined the effects of p27Rex, p21Rex, p30II, and Tax on HTLV-1 derived reporter activity. As shown in Fig. 6A, p27Rex significantly increased HTLV-1 reporter activity, which was very similar to that following NMD inhibition by siUPF1 or siUPF2 (Fig. 2B). p21Rex also significantly elevated HTLV-1 reporter activity, but to a lesser extent compared with p27Rex, whereas p30II and Tax did not significantly influence reporter activity (Fig. 6A). As anticipated from the accrued data and early reports by others [18–20], we also demonstrated that unspliced HTLV-1 mRNA was significantly stabilized in cells containing p27Rex (half-life = 11.3 h) compared with control cells containing empty vectors (half-life = 2.3 h) (Fig. 6B). On the other hand, p30II and Tax did not show significant effects on stabilization of unspliced HTLV-1 mRNA (half-lives = 3.4 h and 2.8 h, respectively). Interestingly, p21Rex, which does not have NLS and hence does not localize to the nucleus, also stabilized unspliced HTLV-1 unspliced mRNA (half-life = 11.0 h). These data further support that stabilization of viral genomic RNA by Rex is, at least partially, achieved by its function in the cytoplasm. Significantly, viral particle production, as determined by HTLV-1 Gag p53 (precursor), p24, and p19 protein expression levels, was increased under conditions of NMD inhibition by antisense-*upf2* mRNA overexpression that suppressed UPF2 protein expression (Fig. 6C). In addition, this increased level of Gag protein, especially in p53 and p19, was comparable to that observed following p27Rex and p21Rex overexpression (Fig. 6D). Given that p27Rex and p21Rex significantly stabilizes HTLV-1 *gag* mRNA (Fig. 6B), these data suggest that Rex enhances HTLV-1 replication by stabilizing unspliced viral transcripts via the suppression of host NMD activity.

4. Discussion

In this study, we demonstrate that HTLV-1 genomic and *gag/pol* RNA is recognized by UPF1, the principal regulator and initiator of NMD, and is thereby targeted for destruction

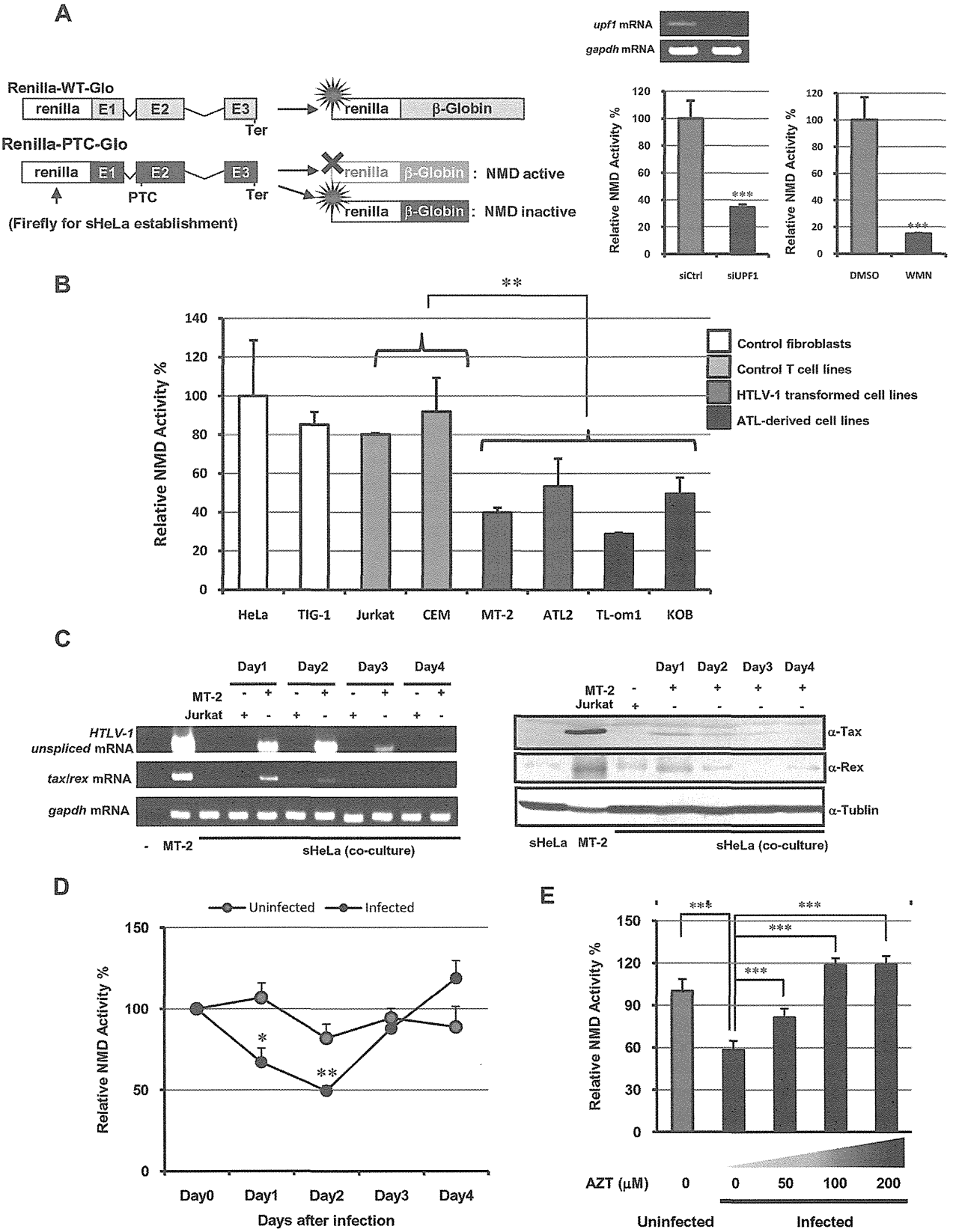

Fig. 3. HTLV-1 infection inhibits cellular NMD activity. (A) A schematic representation of the β-globin NMD reporter plasmids. PTC indicates a premature termination codon and Ter indicates a WT stop signal. The renilla fragment of Renilla-PTC-Glo was replaced with the firefly fragment for establishment of sHeLa cells, which stably expressed both Renilla-WT-Glo and Firefly-PTC-Glo, thus WT-Glo and PTC-Glo expression level was detected as renilla and firefly luciferase activity, respectively. ✸ indicates the luciferase activity. The renilla activity of Renilla-WT-Glo is always active and not influenced by the cellular NMD activity.

by the host NMD machinery. Moreover, we found that HTLV-1 has evolved mechanisms to override and escape the host NMD pathway. We provide evidence that HTLV-1 Rex plays a critical role in the suppression of host NMD activity.

Firstly, we demonstrated that the host-encoded NMD specifically targets HTLV-1 genomic RNA and primary transcripts for RNA turnover. Therefore, host NMD acts to reduce viral structural gene expression and perturbs virus production. The steady-state expression of HTLV-1 unspliced mRNA showed a negative correlation with cellular NMD activity (Fig. 1A), and the stability of unspliced viral mRNA was highly sensitive to cellular NMD activity (Fig. 1B). Luciferase reporter assays, in which the luciferase activity reflects the stability of a *gag*-derived fragment of HTLV-1 genomic RNA, showed that the stability of HTLV-1 *gag* mRNA was directly influenced by the cellular level of UPF1 or UPF2, the key positive regulator of NMD (Fig. 2). Many researchers have demonstrated that UPF1 phosphorylation by the serine/threonine kinase SMG1 facilitates triggering of NMD and exclusion of aberrant mRNAs from the normal translational pathway. These mRNAs are redirected to the P-body, where they await targeted turnover [21,22]. UPF1 plays an important role in discrimination of PTCs that are positioned upstream of EJC at the last exon–exon boundary of spliced mRNAs and selectively activates the NMD machinery for degradation of the targeted mRNA [23]. Recognition of PTC by UPF1 is achieved by interaction of UPF1 at the termination codon with UPF2/UPF3 at EJC, which becomes possible only when a termination codon is positioned upstream of EJC. In yeast, the P-body is the major site for PTC-containing aberrant mRNAs awaiting degradation [24–26]. In mammalian and human cells, all NMD components localize to P-bodies [21] and phosphorylated UPF1 accumulates at these structures [22], supporting the notion that P-bodies accumulate mRNAs targeted for NMD turnover in mammalian cells. Taken together, accumulating evidence indicates that UPF1 is the key regulator in discrimination, selection, and translocation of aberrant mRNAs to P-bodies where they await degradation [21–23,26,27]. The results in the present study demonstrate that phosphorylated UPF1 interacts with HTLV-1 unspliced RNA with a high affinity and the HTLV-1 unspliced RNA complex accumulates in P-bodies (Fig. 1C and D). Our results thus indicate that HTLV-1 genomic RNA is detected by UPF1 as are other cellular NMD target mRNAs and transferred to P-bodies for degradation. Consistent with this notion, NMD antagonized efficient HTLV-1 replication (Fig. 1A and B), whereas the suppression of NMD activity led to a significant increase in HTLV-1 Gag proteins, p53, p24, and p19 (Fig. 6C). Thus, NMD destabilizes HTLV-1 genomic RNA and reduces the expression of viral structural proteins, presumably leading to a reduction in viral particle formation.

Several reports raise the possibility that retroviral transcripts are selectively targeted by the host mRNA decay mechanism, and they have unique or overlapped strategies to avoid degradation. Viral mRNAs of Rous sarcoma virus (RSV) [28] and human foamy virus [29] are selectively degraded in the host cell, although the authors of those studies concluded that the degradation may be accomplished by pathways distinct from NMD. Ajamian et al. reported influence of host encoded NMD-factor, UPF1, on unspliced HIV-1 mRNA, intriguingly enhancing the stability of HIV-1 mRNA [30]. Hogg and Goff proposed a possible model that 3′ UTR-length-dependent accumulation of UPF1 functions as a mark of potential mRNA-decay target [31]. The authors speculated that retroviruses may take advantage of this host-encoded system by employing in-frame read though and/or frame-shifting, which prevents steady-state UPF1 interaction and RNP composition, thus disrupts recognition of the viral mRNA as a decay target. In addition to these previous reports, our data show that unspliced HTLV-1 RNA is a target of a powerful host-encoded mRNA decay mechanism, NMD, and for efficient replication and propagation of new viral particles, it is critical for HTLV-1 to evade the NMD pathway.

On confirming that the host NMD pathway represents a significant impediment to efficient HTLV-1 replication, we posed the critical question: has HTLV-1 evolved a strategy to evade NMD? We observed that HTLV-1-infected cell lines have significantly lower basal NMD activities than HTLV-1-unrelated cell lines (Fig. 3B), implying that HTLV-1 infection may influence host NMD activity. Indeed, the NMD activity was notably suppressed by HTLV-1 infection or protected by inhibition of HTLV-1 infection via AZT treatment (Fig. 3C–E), suggesting the existence of viral factor(s) that suppress the host NMD pathway. Besides the structural proteins, HTLV-1 encodes regulatory and accessory proteins (Tax, Rex, p30II, p12, and p13) in the pX region of the genome. The functions of those proteins have been well studied and reviewed [32,33]. Tax is a multifunctional oncoprotein and transcriptional transactivator that regulates both viral and cellular gene expression [34,35]. HTLV-1 Rex is a virus-encoded, high-affinity, RNA-binding protein that binds

On the other hand, the luciferase activity of PTC-Glo, of which transcript is NMD target, can be detected only under NMD inhibition. The reporter is sensitive to changes in NMD activity in HeLa cells (right panel). Data from three independent experiments are shown ($n = 3$, mean ± SD; $^{***}p < 0.001$). (B) NMD activities were measured by β-globin-based NMD reporter assays in control fibroblasts (HeLa and TIG-1), control T-cell lines (Jurkat and CEM), HTLV-1-transformed cell lines (MT-2 and ATL2), and ATL-derived cell lines (TL-Om1 and KOB). HTLV-1-infected T cell lines show significantly lower NMD activities compared with HTLV-1-unrelated cell lines. Data from three independent experiments are shown ($n = 3$, mean ± SD; $^{**}p < 0.01$). (C) The course of HTLV-1 expression in sHeLa cells co-cultured with MT-2. *Gag* or *tax/rex* mRNA by RT-PCR (left panel) as well as Tax and Rex protein levels determined by Western blotting (right panel) show peaked viral expression 1 and 2 days after infection. (D) NMD activity was measured via dual luciferase assays in HTLV-1 infected sHeLa cells and compared with that in uninfected control cells. Gray circles indicate the results from uninfected control cells, while black circles represent data from HTLV-1 infected cells. Significant NMD inhibition was observed on the first ($p < 0.05$) and second ($p < 0.01$) days after HTLV-1 infection. Results shown are from three independent experiments ($n = 3$, mean ± SE; $^{*}p < 0.05$; $^{**}p < 0.01$). (E) NMD inhibitory effect of HTLV-1 infection is diminished by AZT treatment in HTLV-1 infected sHeLa cells by co-cultivation with MT-2 cells. NMD inhibition by HTLV-1 was abrogated in a dose-dependent manner by AZT treatment ($n = 6$, mean ± SD; $^{***}p < 0.001$).

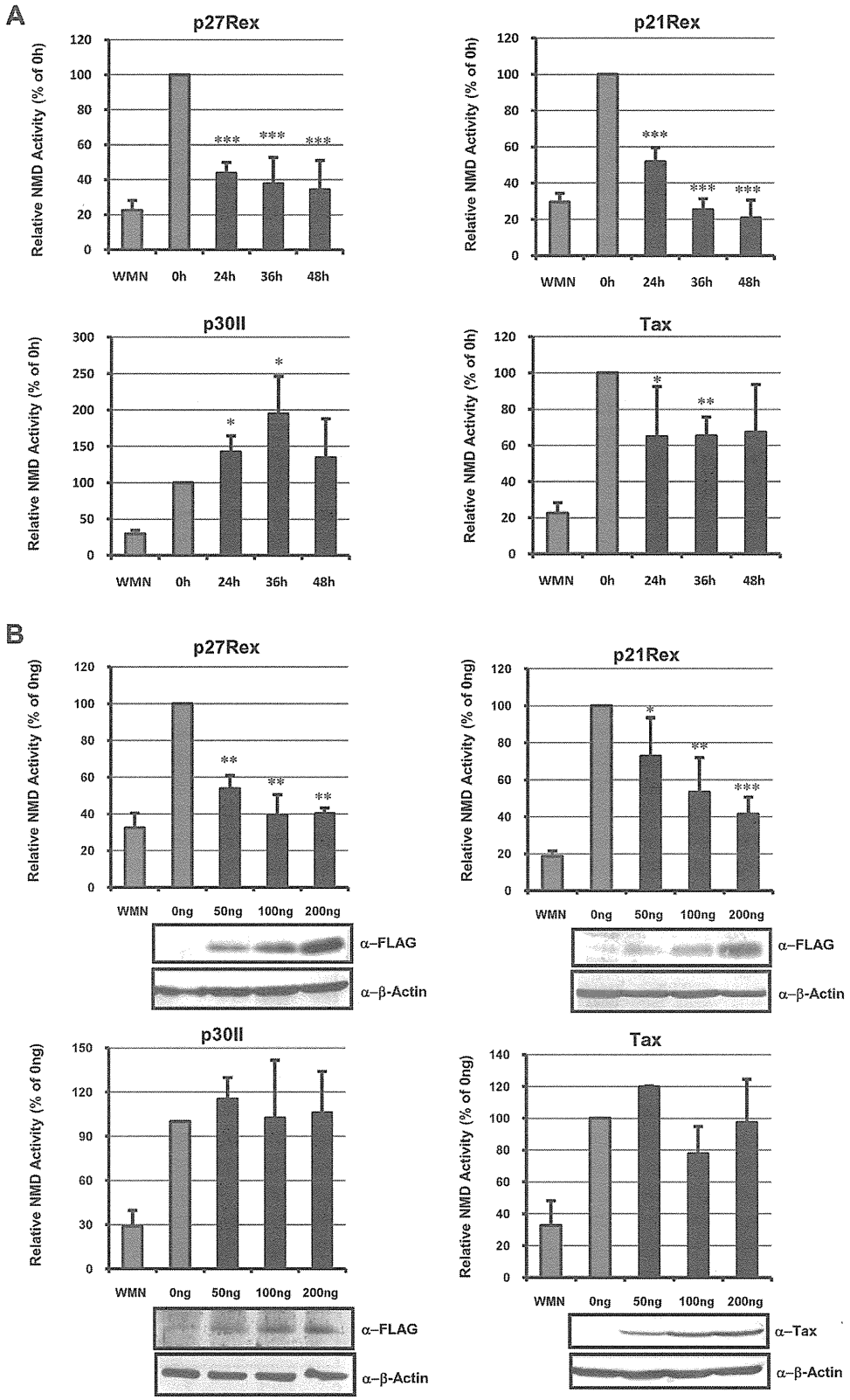

Fig. 4. HTLV-1 Rex is the key viral factor inhibiting NMD. (A) p27Rex and p21Rex inhibit NMD activity in a time-dependent manner, when 200 ng each of viral protein expression plasmid was transfected to sHeLa cells. Tax also demonstrated an NMD inhibitory effect but to a less significant level compared with p27Rex and p21Rex. A representative result from three independent experiments is shown ($n = 3$, mean ± SD; *$p < 0.05$; **$p < 0.01$; ***$p < 0.001$). (B) Both p27Rex and p21Rex suppressed NMD activity in a dose-dependent manner when 50–200 ng of viral protein expression plasmid was transfected to sHeLa cells. A representative result from three independent experiments is shown ($n = 3$, mean ± SD; *$p < 0.05$; **$p < 0.01$; ***$p < 0.001$).

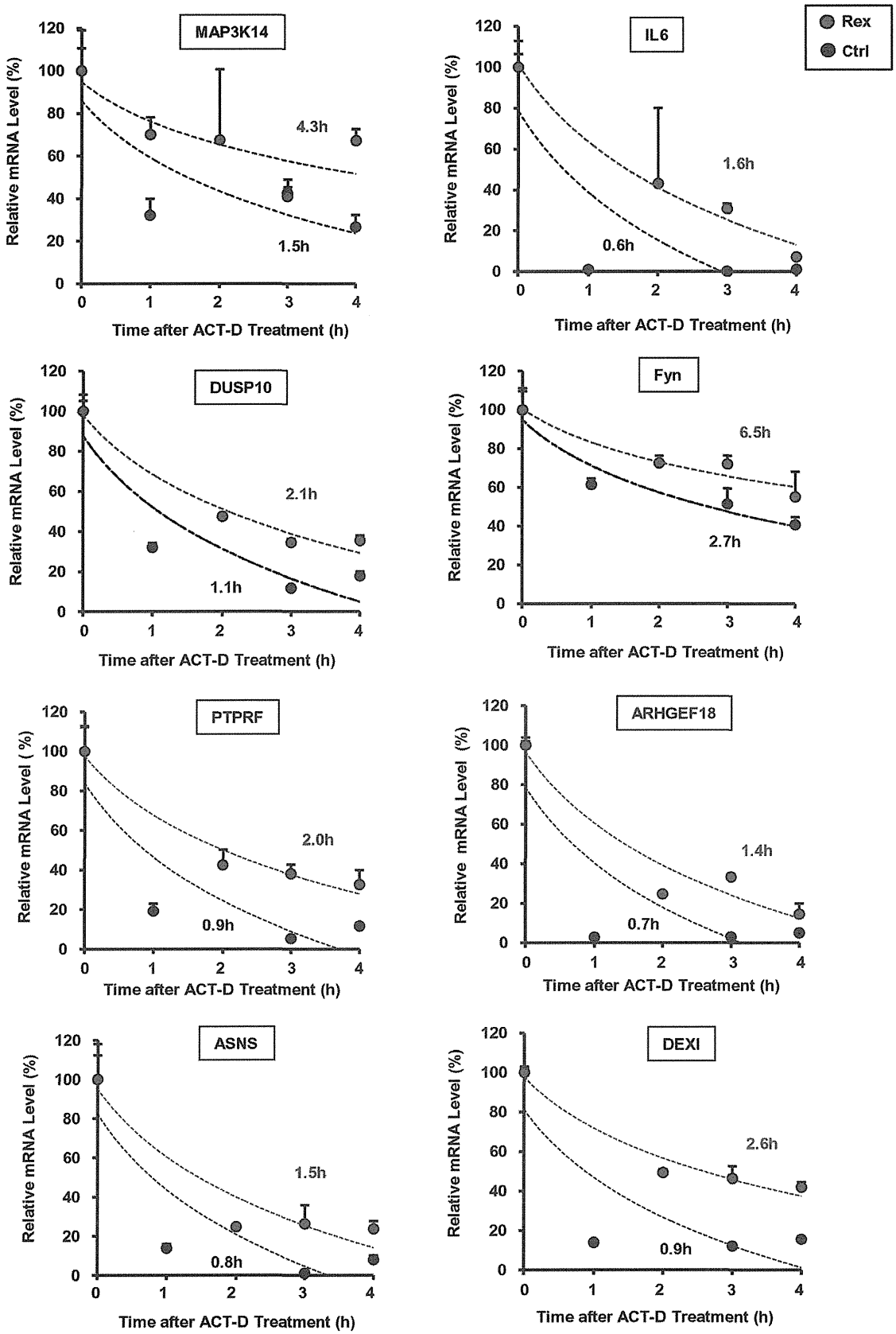

Fig. 5. Rex inhibits global NMD activity. The stability of NMD target mRNAs containing uORFs or 3′ UTR introns as NMD-inducing features [2] were measured in CEM-Rex and CEM-Ctrl. These mRNAs for NMD substrates were significantly stabilized in Rex-overexpressing cells, indicating that Rex represents a general block to global cellular NMD activity. Red circle: CEM-Rex; black circle: CEM-Ctrl. The indicated time is the half-life of tested mRNA calculated based on the regression curve (dashed line).

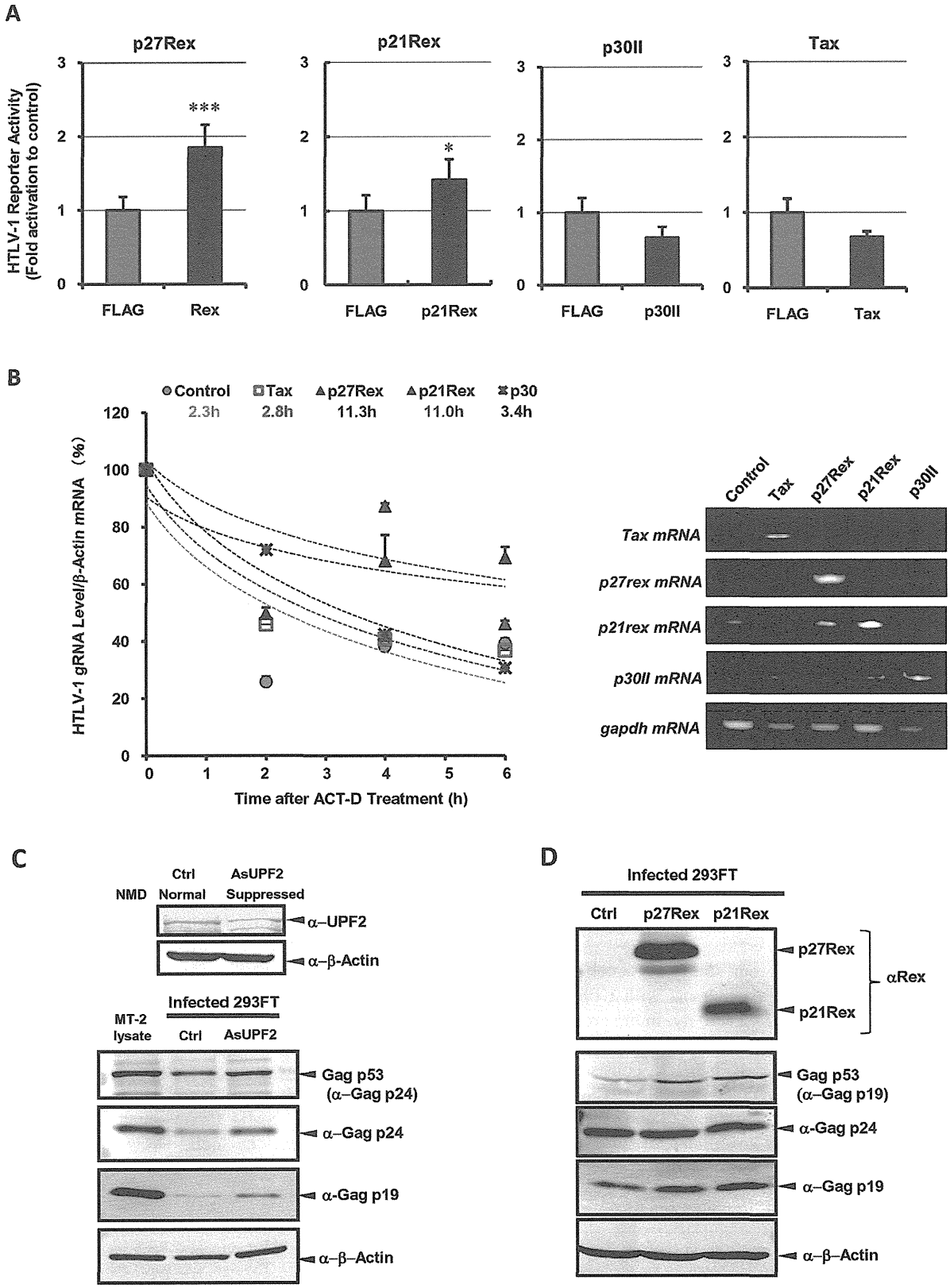

Fig. 6. Rex stabilizes HTLV-1 unspliced mRNA and enhances viral replication via NMD inhibition. (A) The effects of p27Rex, p21Rex, p30II, and Tax on HTLV-1 derived reporter activity in HeLa cells. The reporter activity was significantly increased by p27Rex and p21Rex but not by p30II and Tax ($n = 3–5$, mean ± SD; $*p < 0.05$; $***p < 0.001$). (B) The effect of HTLV-1 regulatory proteins p27Rex (red ▲), p21Rex (purple ▲), p30II (black×), Tax (blue□), and control (green●) on the stability of HTLV-1 genomic unspliced RNA in HTLV-1 infected HeLa cells by co-cultivation with MT-2 cells. HTLV-1 unspliced RNA in p27Rex-overexpressing cells was significantly stabilized (half-life = 11.3 h), followed by stabilization in p21Rex-overexpressing cells (half-life = 11.0 h) compared

to the Rex response element (RxRE) of viral transcripts and promotes selective nuclear export of viral genomic RNA [32,36]. P30II is also an RNA-binding protein that binds mainly to double-spliced *tax/rex* mRNA and reduces translation from this mRNA by retaining it to the nucleolus [37–39]. In a series of experiments testing the influence of these viral factors on NMD activity, only p27Rex and p21Rex displayed a robust time- and dose-dependent inhibition of NMD activity (Fig. 4). The most important and well-studied function of Rex is to promote nuclear export and enhance the stability of unspliced and singly spliced HTLV-1 mRNAs that encode viral structural proteins, by interacting with Rex Responsive Element (RxRE) situated at the 3′ end of all HTLV-1 mRNAs [18,19,40–42], and by engagement with the cellular nuclear export factor CRM1 [18,43,44]. The molecular mechanism of Rex in protection of unspliced viral RNA has not been fully clarified, however, partially explained by active export of mRNA from the nucleus, thereby escaping from the site of splicing. Nevertheless, the fate of viral RNA in the cytoplasm has not been methodically explored. From our data, we propose that Rex assists viral RNA transit within the cytoplasm and ensures efficient translation by subduing NMD and the host mRNA surveillance systems.

We demonstrated that the NMD activity of TL-Om1 cells was significantly suppressed (Fig. 3B), although these cells do not express any of viral proteins at detectable levels. The molecular mechanism of NMD inhibition in TL-Om1 cells is apparently different from that of Rex expressing cells, however, it can be conceived that disturbances of cellular homeostasis caused by HTLV-1 during the early stages of infection, including inhibition of NMD by Rex, might have been conserved after malignant transformation of the infected cells. To gain further insights into the mechanisms, comparative analyses of cell lines that were HTLV-1 immortalized in vitro, such as MT-2, and those derived from ATL and without Rex expression, such as TL-Om1, may provide valuable information as model cells in the early stages of infection and immortalization, and those in the later transformed phase, respectively.

During the completion of our study, Mocquet et al. [45] demonstrated that HTLV-1 Tax interacts with UPF1 and exerts an inhibitory effect on NMD activity. In the present study, Tax also consistently exhibited an inhibitory effect on NMD activity, but both p21Rex and p27Rex consistently outperformed Tax in our assays (Figs. 4 and 6A). Therefore, the studies described here specifically focused on the inhibition of NMD activity exerted by both Rex alleles. In our view, it is not surprising that retroviruses have evolved multiple and overlapping mechanisms to overcome the restrictive properties of NMD. This is especially relevant at early times of viral infection or alternatively, when the provirus is emerging from latency. Under such conditions, there may be insufficient Rex concentration to saturate the NMD pathway. Therefore, another mechanism that augments the NMD inhibitory activity of Rex, such as that presented by Tax, may be required to cooperatively incapacitate NMD. Significantly, recent studies have demonstrated that *tax/rex* mRNAs are the most abundant viral transcripts at early times of infection or following proviral reactivation, and that viral gene expression follows a two-phase pattern that is determined principally by Rex [46].

Our data are consistent with the view that increased luciferase activity of NMD-sensitive reporters by Rex was due to the suppression of overall cellular NMD activity but not due to RxRE-mediated nuclear export of reporter mRNAs by Rex. This is because (1) none of the NMD reporter mRNAs used in this study contain RxRE; (2) the amounts of unspliced and spliced forms of β-globin mRNA in nuclear and cytosolic fractions of the cells were not influenced by Rex expression (Fig. S3A); and (3) the insertion of RxRE after the β-globin fragment of the NMD reporter plasmids had no impact on the NMD inhibitory effect of Rex (Fig. S3B). The data that p21Rex, lacking NLS and RxRE-binding domain at the N-terminal region, is also capable of suppressing NMD strongly support the notion that NMD inhibition is genetically separable from the RxRE-binding function of Rex (Fig. 4). Indeed, we demonstrated that Rex stabilizes a series of NMD target mRNA with NMD-inducing features such as uORFs and 3′ UTR introns (Fig. 5), providing strong evidence that Rex blocks overall cellular NMD activity. On the other hand, it is widely accepted that NMD is involved in cellular homeostasis not only by eliminating PTC-containing aberrant mRNAs but also by controlling the levels of natural transcripts. Approximately 1–10% of eukaryotic transcripts are known to be targeted by NMD because of their potentially NMD-sensitive structures, i.e., PTCs encoded by alternative exons, introns in 3′ UTRs, or uORFs [2,47]. Thus, NMD dysfunction can lead to the destruction of cell homeostasis and may even trigger tumorigenesis [48]. Clearly, overall NMD inhibition by Rex is beneficial to HTLV-1 as a direct mechanism to enhance the stability of HTLV-1 genomic RNA. In contrast, it may perturb cellular gene expression and discrimination of aberrant mRNAs, which are critically regulated by NMD under normal conditions. Indeed, NMD targets many mRNAs, of which products participate in cell cycle regulation, T cell

with that in control cells (half-life = 2.3 h). In contrast, Tax and p30II did not significantly stabilize HTLV-1 unspliced RNA (half-lives = 2.8 and 3.4 h, respectively). The half-life was calculated based on the regression curve (dashed line) ($n = 4$, mean ± SE). The right side panel shows mRNAs levels of *tax*, *p27rex*, *p21rex*, and *p30ii* at 0 h measured by semi-quantitative RT-PCR in HTLV-1 infected cells expressing the indicated viral proteins, ectopically. (C) Expression of HTLV-1 structural proteins, Gag p53 (precursor), p24, and p19, in HTLV-1 infected 293FT cells co-cultured with MT-2 after NMD suppression by As-*upf2* mRNA overexpression to knockdown UPF2 protein expression (top panel). The expression levels of all Gag proteins, p53, p24, and p19, were significantly elevated in the 293FT cells after NMD suppression. (D) The influence of p27Rex and p21Rex on the expression of HTLV-1 Gag structural proteins, p53, p24, and p19, in HTLV-1 infected 293FT cells co-cultured with MT-2. The results showed that the expression levels of HTLV-1 Gag proteins, especially those of Gag p53 and p19, were significantly increased by p27Rex and p21Rex overexpression.

development, and inflammation [2]. The potential pleiotropic impact of Rex mediated through the NMD pathway represents an important and novel aspect of host–retrovirus interaction in viral leukemogenesis.

In conclusion, this study provides evidence that the host-encoded NMD pathway restricts viral RNA expression, thereby reducing HTLV-1. Furthermore, we demonstrated that a novel function for HTLV-1 Rex in inhibition of the host NMD machinery. Rex-mediated inhibition of NMD activity is pleiotropic and may affect both viral and cellular target RNA. Together with the data presented here, there is accumulating evidence of a dynamic interplay between the cellular NMD pathway and pathways for viral gene expression and replication. Clarifying underlying molecular mechanism in inhibition of NMD by Rex is essential to understand this new aspect of host–pathogen interaction. Finally we suggest that the NMD pathway may exert anti-viral effects on other RNA viruses and may participate generally in the innate immune response to viral pathogens. It is therefore likely that other viruses have evolved mechanisms to silence NMD activity during viral infection.

Acknowledgment

This work was supported by Grants-in-Aid for Scientific Research from the Ministry of Education, Culture, Sports, Science, and Technology of Japan, to TW (No. 19659241) and to KN (Nos. 22700863, 24501304).

Appendix A. Supplementary data

Supplementary data related to this article can be found at http://dx.doi.org/10.1016/j.micinf.2013.03.006.

References

[1] R.T. Hillman, R.E. Green, S.E. Brenner, An unappreciated role for RNA surveillance, Genome Biol. 5 (2004) R8.
[2] J.T. Mendell, N.A. Sharifi, J.L. Meyers, F. Martinez-Murillo, H.C. Dietz, Nonsense surveillance regulates expression of diverse classes of mammalian transcripts and mutes genomic noise, Nat. Genet. 36 (2004) 1073–1078.
[3] F.J. Iborra, A.E. Escargueil, K.Y. Kwek, A. Akoulitchev, P.R. Cook, Molecular cross-talk between the transcription, translation, and nonsense-mediated decay machineries, J. Cell Sci. 117 (2004) 899–906.
[4] L.E. Maquat, Nonsense-mediated mRNA decay: splicing, translation and mRNP dynamics, Nat. Rev. 5 (2004) 89–99.
[5] L. Balvay, M.L. Lastra, B. Sargueil, J. Darlix, T. Ohlmann, Translational control of retroviruses, Nat. Rev. 5 (2007) 128–140.
[6] N.J. McGlincy, C.W. Smith, Alternative splicing resulting in nonsense-mediated mRNA decay: what is the meaning of nonsense? Trends Biochem. Sci. 33 (2008) 385–393.
[7] E.P. Plant, P. Wang, J.L. Jacobs, J.D. Dinman, A programmed-1 ribosomal frameshift signal can function as a *cis*-acting mRNA destabilizing element, Nucleic Acids Res. 32 (2004) 784–790.
[8] A.L. Saltzman, Y.K. Kim, Q. Pan, M.M. Fagnani, L.E. Maquat, B.J. Blencowe, Regulation of multiple core spliceosomal proteins by alternative splicing-coupled nonsense-mediated mRNA decay, Mol. Cell Biol. 28 (2008) 4320–4330.
[9] C. Theis, J. Reeder, R. Giegerich, KnotInFrame: prediction of -1 ribosomal frameshift events, Nucleic Acids Res. 36 (2008) 6013–6020.
[10] A.M. Dickson, J. Wilusz, Strategies for viral RNA stability: live long and prosper, Trends Genet. 27 (2011) 286–293.
[11] S. Boelz, G. Neu-Yilik, N.H. Gehring, M.W. Hentze, A.E. Kulozik, A chemiluminescence-based reporter system to monitor nonsense-mediated mRNA decay, Biochem. Biophys. Res. Commun. 349 (2006) 186–191.
[12] T. Ohsugi, T. Kumasaka, T. Urano, Construction of a full-length human T cell leukemia virus type I genome from MT-2 cells containing multiple defective proviruses using overlapping polymerase chain reaction, Anal. Biochem. 329 (2004) 281–288.
[13] N.H. Gehring, G. Neu-Yilik, T.W. Schell, M. Hentze, A.E. Kulozik, Y14 and hUpf3b form an NMD-activating complex, Mol. Cell 11 (2003) 939–949.
[14] Y.K. Kim, L. Furic, L. DesGroseillers, L.E. Maquat, Mammalian staufen1 recruits Upf1 to specific mRNA 3_UTRs so as to elicit mRNA decay, Cell 120 (2005) 195–208.
[15] B. Lee, Y. Tanaka, H. Tozawa, Monoclonal antibody defining Tax1 protein of human T-cell leukemia virus type-I, Tohoku J. Exp. Med. 157 (1989) 1–11.
[16] Y. Tanaka, B. Lee, T. Inoi, H. Tozawa, N. Yamamoto, Y. Hinuma, Antigens related to three core proteins of HTLV-I (p24, p19 and p15) and their intracellular localizations, as defined by monoclonal antibodies, Int. J. Cancer 37 (1986) 35–42.
[17] J. Zhao, B.K. Sun, J.A. Erwin, J. Song, J.T. Lee, Polycomb proteins targeted by a short repeat RNA to the mouse X chromosome, Science 322 (2008) 750–756.
[18] M. Gröne, C. Koch, R. Grassmann, The HTLV-1 Rex protein induces nuclear accumulation of unspliced viral RNA by avoiding intron excision and degradation, Virology 218 (1996) 316–325.
[19] M. Hidaka, J. Inoue, M. Yoshida, M. Seiki, Post-transcriptional regulator (rex) of HTLV-1 initiates expression of viral structural proteins but suppresses expression of regulatory proteins, EMBO J. 7 (1988) 519–523.
[20] J. Inoue, M. Yoshida, M. Seiki, Transcriptional (p40x) and post-transcriptional (p27x-III) regulators are required for the expression and replication of human T-cell leukemia virus type I genes, Proc. Natl. Acad. Sci. U. S. A. 84 (1987) 3653–3657.
[21] A. Eulalio, I. Behm-Ansmant, E. Izaurralde, P-Bodies: at the crossroads of post-transcriptional pathways, Nat. Rev. 8 (2007) 9–22.
[22] T.M. Franks, G. Singh, J. Lykke-Andersen, UPF1 ATPase dependent mRNP disassembly is required for completion of nonsense-mediated mRNA decay, Cell 143 (2010) 938–950.
[23] O. Isken, L.E. Maquat, The multiple lives of NMD factors: balancing roles in gene and genome regulation, Nat. Rev. 9 (2008) 699–712.
[24] R. Parker, U. Sheth, P bodies and the control of mRNA translation and degradation, Mol. Cell 25 (2007) 635–646.
[25] J. Rehwinkel, I. Behm-Ansmant, D. Gatfield, E. Izaurralde, A crucial role for GW182 and the DCP1:DCP2 decapping complex in miRNA-mediated gene silencing, RNA 11 (2005) 1640–1647.
[26] U. Sheth, R. Parker, Targeting of aberrant mRNAs to cytoplasmic processing bodies, Cell 125 (2006) 1095–1109.
[27] L. Unterholzner, E. Izaurralde, SMG7 acts as a molecular link between mRNA surveillance and mRNA decay, Mol. Cell 16 (2004) 587–596.
[28] J.E. Weil, K.L. Beemon, A 3′ UTR sequence stabilizes termination codons in the unspliced RNA of Rous sarcoma virus, RNA 12 (2007) 102–110.
[29] E.G. Lee, D. Kuppers, M. Horn, J. Roy, C. May, M.L. Linial, A premature termination codon mutation at the C terminus of foamy virus *gag* downregulates the levels of spliced *pol* mRNA, J. Virol. 82 (2008) 1656–1664.
[30] L. Ajamian, L. Abrahamyan, M. Milev, P.V. Ivanov, A.E. Kulozik, N.H. Gehring, A.J. Mouland, Unexpected roles for UPF1 in HIV-1 RNA metabolism and translation, RNA 14 (2008) 914–927.
[31] J.R. Hogg, S.P. Goff, UPF1 senses 3′ UTR length to potentiate mRNA decay, Cell 143 (2010) 379–389.
[32] O.U. Susova, V.E. Gurtsevich, The role of region pX in the life cycle of HTLV-I and in carcinogenesis, Mol. Biol. 37 (2003) 334–344.
[33] G. Franchini, R. Fukumoto, J.R. Fullen, T-cell control by human T-cell leukemia/lymphoma virus type-1, Int. J. Hematol. 78 (2003) 280–296.
[34] M. Boxus, J.-C. Twizere, S. Legros, J.-F. Dewulf, R. Kettmann, L. Willems, The HTLV-1 Tax interactome, Retrovirology 5 (2008) 76.

[35] F. Kashanchi, J.N. Brady, Transcriptional and post-transcriptional gene regulation of HTLV-1, Oncogene 24 (2005) 5938–5951.
[36] I. Younis, P.L. Green, The human T-cell leukemia virus Rex protein, Front. Biosci. 10 (2005) 431–445.
[37] C. Nicot, M. Dundr, J.M. Johnson, J.R. Fullen, N. Alonzo, R. Fukumoto, G.L. Princler, D. Derse, T. Misteli, G. Franchini, HTLV-1-encoded p30II is a post-transcriptional negative regulator of viral replication, Nat. Med. 10 (2004) 197–201.
[38] U. Sinha-Datta, A. Datta, S. Ghorbel, M. Duc Dodon, C. Nicot, Human T-cell lymphotrophic virus type I Rex and p30 interactions govern the switch between virus latency and replication, J. Biol. Chem. 282 (2007) 14608–14615.
[39] H.H. Baydoun, M. Bellon, C. Nicot, HTLV-1 yin and yang: Rex and p30 master regulators of viral mRNA trafficking, AIDS Rev. 10 (2008) 195–204.
[40] Y.F. Ahmed, G.M. Gilmartin, S.M. Hanly, J.R. Nevins, W.C. Greene, Structure–function analyses of the HTLV-I Rex and HIV-1 Rev RNA response elements: insights into the mechanism of Rex and Rev action, Gene Develop. 4 (1990) 1014–1022.
[41] Y.F. Ahmed, G.M. Gilmartin, S.M. Hanly, J.R. Nevins, W.C. Greene, The HTLV-I Rex response element mediates a novel form of mRNA polyadenylation, Cell 64 (1991) 727–737.
[42] Y. Adachi, T. Nosaka, M. Hatanaka, Protein kinase inhibitor H-7 blocks accumulation of unspliced mRNA of human T-cell leukemia virus type I (HTLV-I), Biochem. Biophys. Res. Commun. 169 (1990) 469–475.
[43] Y. Hakata, T. Umemoto, S. Matsushita, H. Shida, Involvement of human CRM1 (exportin 1) in the export and multimerization of the Rex protein of human T-cell leukemia virus type 1, J. Virol. 72 (1998) 6602–6607.
[44] Y. Hakata, M. Yamada, Rat CRM1 is responsible for the poor activity of human t-cell leukemia virus type 1 Rex protein in rat cells, J. Virol. 75 (2001) 11515–11525.
[45] V. Mocquet, J. Neusiedler, F. Rende, D. Cluet, J.-P. Robin, J.-M. Terme, M. Duc Dodon, J. Wittmann, C. Morris, H.L. Hir, V. Ciminale, P. Jalinot, The human t-lymphotropic virus type 1 Tax protein inhibits nonsense-mediated mRNA decay by interacting with INT6/EIF3E and UPF1, J. Virol. 86 (2012) 7530–7543.
[46] F. Rende, I. Cavallari, A. Corradin, M. Silic-Benussi, F. Toulza, G.M. Toffolo, Y. Tanaka, S. Jacobson, G.P. Taylor, D.M. D'Agostino, C.R.M. Bangham, V. Ciminale, Kinetics and intracellular compartmentalization of HTLV-1 gene expression: nuclear retention of HBZ mRNAs, Blood 117 (2011) 4855–4859.
[47] P. Nicholson, H. Yepiskoposyan, S. Metze, R.Z. Orozco, N. Kleinschmidt, O. Mühlemann, Nonsense-mediated mRNA decay in human cells: mechanistic insights, functions beyond quality control and the double-life of NMD factors, Cell. Mol. Life Sci. 67 (2010) 677–700.
[48] L.B. Gardner, Nonsense-mediated RNA decay regulation by cellular stress: implications for tumorigenesis, Mol. Cancer Res. 8 (2010) 295–308.

AIDS RESEARCH AND HUMAN RETROVIRUSES
Volume 29, Number 5, 2013
© Mary Ann Liebert, Inc.
DOI: 10.1089/aid.2012.0205

Altered Expression of Degranulation-Related Genes in CD8$^+$ T Cells in Human T Lymphotropic Virus Type I Infection

Tathiane M. Malta,[1,2] Israel T. Silva,[1] Daniel G. Pinheiro,[1] Anemarie R.D. Santos,[1] Mariana T. Pinto,[1,2] Rodrigo A. Panepucci,[1,3] Osvaldo M. Takayanagui,[3] Yuetsu Tanaka,[4] Dimas T. Covas,[1,3] and Simone Kashima[1,2]

Abstract

Human T lymphotropic virus type I (HTLV-1) is the etiological agent of HTLV-1-associated myelopathy/tropical spastic paraparesis (HAM/TSP). CD8$^+$ T cells may contribute to the protection or development of HAM/TSP. In this study we used SAGE methodology to screen for differentially expressed genes in CD8$^+$ T cells isolated from HTLV-1 asymptomatic carriers (HAC) and from HAM/TSP patients to identify genes involved in HAM/TSP development. SAGE analysis was conducted by pooling samples according to clinical status. The comparison of gene expression profiles between HAC and HAM/TSP libraries identified 285 differentially expressed tags. We focus on cytotoxicity and cytokine-related genes due to their potential biological role in HTLV-1 infection. Our results showed that patients with HAM/TSP have high expression levels of degranulation-related genes, namely GZMH and PRF1, and of the cytoskeletal adaptor PXN. We found that GZMB and ZAP70 were overexpressed in HTLV-infected patients compared to the noninfected group. We also detected that CCL5 was higher in the HAM/TSP group compared to the HAC and CT groups. Our findings showed that CD8$^+$ T cells of HAM/TSP patients have an inflammatory and active profile. PXN and ZAP70 overexpression in HTLV-1-infected patients was described for the first time here and reinforces this concept. However, although active and abundant, CD8$^+$ T cells are not able to completely eliminate infected cells and prevent the development of HAM/TSP and, moreover, these cells might contribute to the pathogenesis of the disease by migrating to the central nervous system (CNS). These results should be further tested with biological functional assays to increase our understanding on the role of these molecules in the development of HTLV-1-related diseases.

Introduction

It is estimated that 20 million people worldwide are infected with human T lymphotropic virus type I (HTLV-1),[1] the etiological agent of adult T cell leukemia/lymphoma (ATLL),[2,3] HTLV-1-associated myelopathy/tropical spastic paraparesis (HAM/TSP),[4,5] and several inflammatory diseases.[6–8] However, only 2–5% of infected individuals will develop ATLL or HAM/TSP, while most will remain asymptomatic throughout life.[9,10] The mechanisms that lead to the development of disease are not fully understood.

HAM/TSP is characterized by chronic and progressive inflammation of the central nervous system (CNS) in which the immune response appears to play an important role during disease development. Immune response is one of the factors that determine proviral load (PVL) and hence the risk of developing HAM/TSP.[11] Most genotypic studies on HTLV-1 show no association between genetic variants of the virus and the risk of developing HAM/TSP.[12,13] However, studies on the polymorphisms in genes related to the production of inflammatory interleukins and DC-sign receptors,[13–15] done in HTLV-1-infected individuals, have found an association between disease susceptibility and/or development. Additionally, the high PVL, the invasion of infected cells to other compartments, and the low efficiency of the host immune response are factors also related to HAM/TSP development.[12,16]

[1]National Institute of Science and Technology in Stem Cell and Cell Therapy, Center for Cell Therapy and Regional Blood Center, Blood Center of Ribeirão Preto, Ribeirão Preto, São Paulo, Brazil.
[2]Faculty of Pharmaceutical Sciences, University of São Paulo, Ribeirão Preto, São Paulo, Brazil.
[3]Faculty of Medicine, University of São Paulo, Ribeirão Preto, São Paulo, Brazil.
[4]Department of Immunology, Graduate School of Medicine, University of the Ryukyus, Nishihara, Okinawa, Japan.

In fact, during HTLV-1 infection immune cells are strongly activated, mainly CD4+ and CD8+ T cells.[17,18] This increased immune response may contribute to tissue damage, as observed in the CNS of subjects who develop HAM/TSP.[19] It is unclear whether HTLV-1-specific CD8+ T cells are responsible for protecting against HAM/TSP by controlling PVL or they are the cause of the inflammatory disease themselves.[20] Nevertheless, these two mechanisms are not mutually exclusive.

As the immune response against HTLV-1 is regulated by many genes, differences in gene expression profiles of CD8+ T cells may contribute to the protection or development of HAM/TSP. Here we looked for differentially expressed genes in CD8+ T cells isolated from asymptomatic HTLV-1-infected individuals and individuals with HAM/TSP, in an attempt to identify genes involved in the development of HAM/TSP. A better knowledge of the molecular mechanisms involved in HTLV-1 infection may provide a better understanding of the regulatory network related to HTLV-1-associated diseases.

Materials and Methods

Patients and controls

HTLV-1 patients belong to the positive serology profile of blood donors of the Regional Blood Center of Ribeirão Preto, São Paulo, Brazil and of patients from the Neurology Department of the Clinical Hospital of the Faculty of Medicine of the University of São Paulo, Ribeirão Preto, Brazil. The diagnosis of HTLV-1 was established by antibody screening of serum/plasma samples using an enzyme immunoassay (rp21e-enhanced EIA; Cambridge Biotech), followed by in house polymerase chain reaction (PCR) confirmation for *tax* and LTR.[21] The study was approved by the Institutional Ethics Committee (process number 3083/2007) and all patients signed an informed consent before enrollment. A total of 40 ml of peripheral blood was obtained from HTLV-1 patients and healthy volunteers. A total of 83 samples were collected. The subjects were divided into three groups: (1) the control group (CT) composed by 40 non-HTLV-1-infected individuals; (2) the asymptomatic group (HAC) composed of 24 HTLV-1-asymptomatic carriers; (3) and the HAM/TSP group (HAM/TSP) with 19 patients. All HTLV-1-seropositive individuals were evaluated for clinical status according to the criteria previously described for ATLL and HAM/TSP.[22] None of the HTLV-1-seropositive individuals showed positive serology for other relevant blood-borne pathogens including hepatitis B virus, hepatitis C virus, human immunodeficiency virus, HTLV-2, Chagas disease, and syphilis. Individuals included in the control group who were blood donors also showed negative serology for these pathogens. Individuals who were not blood donors were screened for HTLV-1 infection and we applied an oral questionnaire in order to search for other infections and for any drug treatment. The individuals who reported any infection or antiinflammatory treatment were excluded from the study. All individuals were evaluated for white blood cell (WBC) count and CD4+ and CD8+ T cell counts. The mean age was around 42.0 (range from 20 to 71) and 55.0 (range from 34 to 75) years old for the HAC and HAM/TSP groups, respectively. Of the HAM/TSP group 84.2% was composed of infected females, whereas 54.2% of the HAC group was composed of females. Of the CT group 75% was composed of women and the mean age was 43.2 years old (range from 22 to 76). The sex and age distribution of the sample groups are shown in Table 1.

Proviral load

The white cell layer was isolated by centrifugation at $900 \times g$ for 10 min at 4°C and transferred to sterile 15-ml polypropylene tubes. DNA was extracted from the buffy coat using a Super Quick Gene DNA Isolation kit (Analytical Genetic Testing Center, Denver, CO). After extraction, HTLV-1 PVL was determined by the quantitative PCR method using ABI Prism 7500 (Applied Biosystems) with 200 ng genomic DNA (roughly equivalent to 10^5 cells).

The reaction mixture was prepared using TaqMan Universal PCR Master Mix (Applied Biosystems) technology to amplify HTLV-1 *tax* and human actin beta (ACTB) genes. The primer set for the HTLV-I *tax* region was 5′-CGG ATA CCC IGT CTA CGT GTT T-3′ and 5′-CTG AGC IGA IAA CGC GTC CA-3′ and the TaqMan fluorescent probe for the *tax* gene was 5′-ATC ACC TGG GAC CCC ATC GAT GGA-3′.[23] To amplify the ACTB region we used the TaqMan Gene Expression Assays–Hs03023880_g1 (Applied Biosystems). The PCR conditions for *tax* amplification were 6.25 μl of the TaqMan Universal PCR Master Mix, 5 μM of each primer, and 5 μM of probe (Applied Biosystems). For ACTB amplification the reaction conditions were 5.0 μl of TaqMan Universal PCR Master Mix and 0.5 μl of probe. The thermal cycler settings were 50°C for 2 min, 95°C for 10 min, and 40 cycles at 95°C for 15 s and 60°C for 1 min. DNA standards were extracted from the MT-2 cell line to make a standard curve. Based on the standard curve created by six concentrations of template (10^1 to 10^6 copies), the concentrations of unknown samples were determined. The amount of HTLV-1 proviral DNA was calculated by the following formula: copy number of HTLV-1 *tax* per 1×10^5 PBMCs = [(copy number of *tax*)/(copy number of ACTB)] $\times 2 \times 10^5$. All samples were duplicated.

CD8+ T cell separation

Peripheral blood mononuclear cells (PBMCs) were separated from whole blood using the Ficoll-Paque PLUS density gradient (GE Healthcare Bio-Sciences AB, Uppsala, Sweden) and stored in fetal bovine serum (FBS) containing 10% dimethyl sulfoxide (DMSO) at N_2 for posterior stained and flow cytometry analysis. CD8+ T cells were isolated using anti-CD8 Ab-coated microbeads by passing PBMCs through a magnetic cell separation system (MACS; Miltenyi Biotec, Bergish Glabach, Germany) with column type LS. The positively selected cells were confirmed as being CD8+ T cells by flow cytometry analysis (FACSCalibur, Becton & Dickinson, San Jose, CA).

Tax expression

PBMCs isolated from 14 HAC and 11 HAM/TSP patients were stained with anti-Tax and analyzed by flow cytometry to quantify the amount of cells that are capable of expressing Tax. PBMCs were cultured in RPMI-1640 medium (Sigma-Aldrich) supplemented with 10% of FBS, 2 mmol/liter glutamine, 100 IU/ml penicillin, 100 μg/ml streptomycin, and 20 nmol/liter concanamycin A (CMA) (Sigma-Aldrich) for 14 h. Harvested cells were washed with phosphate-buffered saline (PBS) and stained with antihuman-CD4-phycoerythrin

Table 1. Descriptive Characteristics of the Control Group, Human T Lymphotropic Virus Type I-Asymptomatic Carriers, and Human T Lymphotropic Virus Type I-Associated Myelopathy/Tropical Spastic Paraparesis Patients According to Clinical Status, Age, Gender, Proviral Load, White Blood Cell Count, and CD4/CD8 Ratio

		Gender (%)				
	Mean age	*F*	*M*	*Proviral load mean (copy number/10^5 cells)*	*White blood cell count (cells/mm^3)*	*CD4/CD8 ratio (mean values)*
CT ($n=40$)	43.2	75.0	25.0	—	7,291	2.06
HAC ($n=24$)	42.0	54.2	45.8	173.5	6,782	1.95
HAM/TSP ($n=19$)	55.0	84.2	15.8	1,075.1	7,272	2.34

F, female; M, male; CT, control group; HAC, HTLV-1-asymptomatic carriers; HAM/TSP, HTLV-1-associated myelopathy/tropical spastic paraparesis.

(PE), antihuman-CD8-PE, and anti-human-CD3-Peridinin Chlorophyll Protein (PerCP) (Becton & Dickinson). Cells were fixed in PBS 1×containing 4% (v/v) paraformaldehyde (Sigma-Aldrich) for 20 min and resuspended in PBS. Fixed cells were washed with PBS containing 4% normal goat serum (Sigma-Aldrich) and permeabilized with PBS containing 0.1% (v/v) Triton X-100 (Sigma-Aldrich) for 7 min at room temperature. Permeabilized cells were washed, resuspended in PBS/4% normal goat serum containing an anti-Tax MAb (Lt-4),[24] and incubated for 30 min. After washing, Alexa Fluor 488-conjugated antimouse IgG3 serum (Invitrogen, Carlsbad, CA) was used as the second antibody for labeling anti-Tax. Finally, the cells were washed twice, analyzed by flow cytometry (FACSCalibur, Becton & Dickinson), and the proportion of $CD8^+$ T cells positive for Tax protein was estimated, indicating the number of $CD8^+$ T cells infected by HTLV-1 capable of expressing the Tax protein.

SAGE procedure

Analysis of the SAGE global gene expression profile was conducted by pooling samples according to clinical status into the HAC and HAM/TSP groups. Each pool was composed by equal amounts of RNA of four individuals whose $CD8^+$ T cells purity was above 80%. Thus, the HAC group was composed of HAC 01, HAC 09, HAC 10, and HAC 11 samples. The HAM/TSP group was composed of HAM/TSP 01, HAM/TSP 05, HAM/TSP 08, and HAM/TSP 09 (Table 2). Total RNA was isolated from $CD8^+$ T cells using TRIzol LS Reagent (Invitrogen) according to the manufacturer's instructions. Twenty-five micrograms of total RNA was used for the SAGE procedure carrying out the I-SAGE Kit (Invitrogen) based on the original SAGE.[25] Amplified inserts were sequenced with forward M13 primer in a MegaBACE 1000 sequencer and the DYEnamic ET Dye Terminator Sequencing Kit (Amersham Biosciences, Piscataway, NJ).

SAGE analysis

HAC and HAM/TSP SAGE tags were extracted from concatamer sequences and analyzed by SAGE 2000 software, version 4.5 (www.sagenet.org), using default parameters. Tag-to-gene assignments were performed based on the CGAP SAGE Genie database ("Hs_short.best_gene" at http://cgap.nci.nih.gov/SAGE). SAGE libraries from the HAC and HAM/TSP groups can be found at the NCBI GEO database numbers GSM641893 and GSM641894, respectively. To compare the gene expression among libraries, the number of tags was normalized to a total count of 300,000 tags. Tags identified as contaminants or technical artifacts were filtered using S3T analysis.[26] The Audic and Claverie significance test[27] and a Fold-Change (FC) criterion were used to identify differently expressed genes (DEG) between libraries (p value <0.01 and $FC>2$). We also estimated the false discovery

Table 2. Descriptive Characteristics of Human T Lymphotropic Virus Type I-Asymptomatic Carriers and Human T Lymphotropic Virus Type I-Associated Myelopathy/Tropical Spastic Paraparesis Patients Included in SAGE Libraries, According to Clinical Status, Gender, Age, Proviral Load, White Blood Cell Count, CD4/CD8 Ratio, and Purity of $CD8^+$ T Cells

Clinical status	*Gender*	*Age (years)*	*Proviral load (copy number/10^5 cells)*	*White blood cell count (cells/mm^3)*	*CD4/CD8 (ratio)*	*Purity $CD8^+$*
HAC 01	F	52	17.7	7,400	1,224/697 (1.76)	82.26%
HAC 09	F	47	50.4	5,900	676/512 (1.32)	90.57%
HAC 10	F	21	15.3	7,100	875/529 (1.65)	91.19%
HAC 11	M	38	321.6	6,400	1,299/538 (2.41)	90.99%
Mean		39.5	101.2	6,700	(1.79)	
HAM/TSP 01	F	34	300.8	7,600	717/378 (1.90)	87.93%
HAM/TSP 05	F	53	888.1	7,100	2,497/1,001 (2.49)	84.56%
HAM/TSP 08	M	55	1,091.4	8,200	ND	98.90%
HAM/TSP 09	M	55	995.3	3,700	468/355 (1.32)	89.86%
Mean		49.3	818.9	6,650	(1.90)	

F, female; M, male; HAC, HTLV-1-asymptomatic carriers; HAM/TSP, HTLV-1-associated myelopathy/tropical spastic paraparesis; ND, not determined.

rate (FDR) in order to evaluate the genes with differential expression.[28] The set of DEG was selected for functional analysis, using annotation databases from Gene Ontology, KEGG, and BioCarta, providing, respectively, the identification of biological processes and interactions of genes into pathways. The DEG was also submitted to Ingenuity Pathway Analysis (IPA) (Ingenuity Systems, www.ingenuity .com). For gene expression analysis, we also used public SAGE libraries from leukocytes obtained from venous blood of normal healthy volunteers[29] (accession number GSE5833).

Real-time quantitative PCR

For qRT-PCR analysis, we studied a total of 55 samples, including the eight samples used to prepare SAGE libraries. Of the total, 24 were CT individuals, 17 were HAC, and 14 had HAM/TSP.

The RNA was reverse transcribed using a High Capacity cDNA Reverse Transcription Kit (Applied Biosystems). Real-time quantitative PCR was conducted in the cDNA of 55 individuals (unpooled) and was performed in 7,500 Real-Time PCR System (Applied Biosystems) using TaqMan Gene Expression Assays (Applied Biosystems) as recommended by the manufacturer. Primers (Applied Biosystems) for the following functionally diverse set of genes were used: perforin 1 (PRF1) (Hs00169473_m1), granzyme B (GZMB) (Hs0018051_m1), granzyme H (GZMH) (Hs00277212_m1), chemokine (C–C motif) ligand 5 (CCL5) (Hs00174575_m1), zeta-chain (TCR)-associated protein kinase 70 kDa (ZAP70) (Hs00896347_m1), and paxillin (PXN) (Hs01104424_m1). The amount of mRNA for each sample was normalized using the geometric average of the two housekeeping genes GAPDH (4310884-E) and RPL13A (185720330-7).[30] All the reactions were duplicated and PCR amplification efficiency was established for all genes and ranged from 0.9 to 1.1. The relative expression levels were calculated using the $2^{-\Delta\Delta Ct}$ method[31] and the median of the CT group was used as the calibrator.

Quantitative flow cytometry analysis

PBMCs were analyzed by quantitative flow cytometry for PRF1 and GZMB. Frozen PBMCs were used for intracellular staining of PRF1 and GZMB. A total of nine uninfected individuals, 15 and 14 patients from the HAC and HAM/TSP groups, respectively, were analyzed. Samples were thawed and washed with PBS and stained with antihuman-CD8-FITC or antihuman-CD8-PE, and with antihuman-CD3-PerCP (Becton & Dickinson). Cells were fixed in PBS containing 4% (v/v) paraformaldehyde (Sigma-Aldrich) and permeabilized with PBS containing 0.1% (v/v) Triton X-100 (Sigma-Aldrich). After washing, the cells were incubated with antihuman-PRF1-clone δG9 anti-PRF1-PE or anti-GZMB-FITC (Becton & Dickinson). Finally, the cells were washed and analyzed by flow cytometry (FACSCalibur, Becton & Dickinson). The mean fluorescence intensity (MFI) was determined, indicating the protein expression level.

Statistical analyses

The statistical analyses to compare the differences in PVL between the HAC and HAM/TSP groups were performed using the Mann–Whitney test. The Mann–Whitney test was also used to evaluate the differences in gene expression quantification between the two groups. Data related to expression levels among three groups were compared by ANOVA followed by Tukey post hoc analyses. To draw correlations between PVL and gene expression we used the nonparametric Spearman test. The statistical analyses were performed using SPSS software version 14. Values of p lower than 0.05 were considered statistically significant.

Results

Epidemiological and clinical features of HTLV-1-infected patients

A total of 83 individuals were tested; of them, 40 were CT individuals, 24 were HAC, and 19 had HAM/TSP. The values of WBC ranged from 2,800 to 12,500 cells/mm^3 but the mean value was similar among groups (Table 1). Nine samples (CT 03, CT 07, CT 08, CT 17, HAC 20, HAM/TSP 03, HAM/TSP 06, HAM/TSP 09, and HAM/TSP 15) showed a WBC count below the reference value whereas five samples (CT 05, CT 22, CT 39, HAM/TSP 12, and HAM/TSP 17) had higher values. For CD4$^+$ and CD8$^+$ count, the values were similar among groups (Table 1), ranging from 1.02 to 4.94. Three individuals (CT 16, HAC 15, and HAM/TSP 11) showed a CD4$^+$/CD8$^+$ ratio below 1.2. The PVL in the HAM/TSP group was six times higher (mean 1,075.1 copy number/10^5 cells) than in the HAC group (mean 173.5 copy number/10^5 cells) ($p < 0.05$) (Table 1).

The proportion of CD8$^+$ T cells infected by HTLV-1, evidenced by the Tax protein expression, was 2.2 times higher in

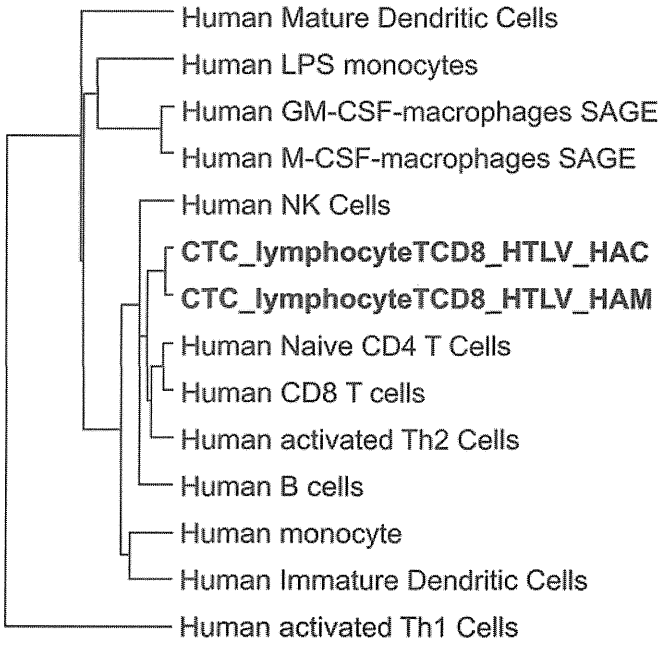

FIG. 1. Hierarchical clustering of leukocytes, dendritic cells, macrophages, and CD8$^+$ T cells isolated from human T lymphotropic virus type I (HTLV-1)-infected individuals. Briefly, a dendrogram was generated by pairwise average linkage (Euclidean distance) using Cluster 3.0 software. Myeloid and lymphoid cells were differentially clustering. CD8$^+$ T cell libraries derived from HTLV-1-infected individuals were grouped together in the lymphoid cluster.